

REGULATION OF CELL SHAPE DURING
DEVELOPMENT OF THE NERVOUS SYSTEM

By

Molly J. Harding

A DISSERTATION

Presented to the Neuroscience Graduate Program
and the Oregon Health & Science University
School of Medicine
in partial fulfillment of
the degree requirements for the degree of

Doctor of Philosophy

September 2013

School of Medicine
Oregon Health & Science University

CERTIFICATE OF APPROVAL

This is to certify that the Ph.D. dissertation of
MOLLY HARDING
has been approved on September 4, 2013

Advisor, Alex Nechiporuk, PhD

Member and Chair, Teresa Nicolson, PhD

Member, Philip Copenhaver, PhD

Member, Philip Stork, MD, PhD

Member, Anthony Barnes, PhD

Member, Mary Logan, PhD

TABLE OF CONTENTS

I. Abstract	1
II. Introduction	3
Figures 1-2	18
III. Chapter 1: Fgfr-Ras-MAPK signaling is required for apical constriction via apical positioning of Rho-associated kinase during mechanosensory organ formation	20
Abstract	21
Introduction	22
Materials and Methods	24
Results	26
Discussion	32
Conclusion	36
Figures 1.1-1.11	38
IV. Chapter 2: Jip-3-dependent Ret localization is required for proper axon extension during peripheral neuron development	50
Abstract	51
Introduction	52
Materials and Methods	56
Results	59
Discussion	65

Conclusion	70
Figures 2.1-2.9	71
V. Chapter 3: Conclusion and Future Directions.....	80
V. References	85

ACKNOWLEDGEMENTS

I thank Philip Stork, Hillary McGraw and Maya Culbertson for their comments on the manuscript presented in Chapter 1. I am also grateful to the OHSU Advanced Light Microscopy Core and Aurelie Snyder for assistance in image analysis and training on *Imaris*. This work was supported by funds from NIH and March of Dimes to A.V.N. and NSF GRF to M.J.H.

I thank Catherine Drerup for her work on the collaborative project presented in Chapter 2. Her intellectual and experimental contributions have greatly improved the project. This work was supported by funds from NIH to A.V.N. and NSF GRF to M.J.H.

I am thankful to all the members of the Nechiporuk Lab, past and present, for creating a stimulating intellectual environment. These individuals include Alex Nechiporuk, Maya Culbertson, Catherine Drerup, Hillary McGraw, Austin Forbes, Zachary Lewis and Chris Riso.

I am grateful to the members of the Neuroscience Graduate Program faculty; In particular, I thank my thesis advisory committee, chairwoman Teresa Nicolson, Philip Stork, Philip Copenhaver and Anthony Barnes, for their continuous support and input on my dissertation work. I also thank Mary Logan for acting as an *ad hoc* member of my dissertation committee.

ABBREVIATIONS

CNS- central nervous system

DMSO- Dimethyl sulfoxide

ERK- Extracellular signal-regulated kinase

Fgf- Fibroblast Growth Factor

FgfR- Fibroblast Growth Factor Receptor

GDNF- glial cell derived neurotrophic factor

hpf- hours post fertilization

Jip3- cJun N-terminal Kinase-interacting protein 3

MAPK- Mitogen-activated protein kinase

MRLC- Myosin Regulatory Light Chain

NGF- nerve growth factor

NM- neuromast

pLL- posterior lateral line

pLLg- posterior lateral line ganglion

pLLp- posterior lateral line primordium

Ras- rat sarcoma

Ret- rearranged in transfection

Rock- Rho-kinase

TrkB- Tropomyosin receptor kinase B

LIST OF FIGURES

Introduction

Figure 1: Mechanosensory hair cells and development of the posterior lateral line.

Figure 2: Development of the posterior lateral line.

Chapter 1

Figure 1.1: Fgf-Ras-MAPK signaling in the pLLp is required for rosette formation.

Figure 1.2 Inhibition of MAPKK phenocopies loss of FgfR signaling.

Figure 1.3: FgfR, Ras and MAPK synergize during formation of the posterior lateral line.

Figure 1.4: FgfR-Ras-MAPK signaling is required for apical constriction.

Figure 1.5 FgfR-Ras-MAPK signaling does not disrupt localization of polarity molecules or the acto-myosin cytoskeleton.

Figure 1.6: Myosin-II is required for rosette formation.

Figure 1.7 Rho-kinase activity is required for rosette formation, apical constriction and MRLC activation.

Figure 1.8 MAPK does not regulate levels and distribution of rock2a transcript in the pLLp.

Figure 1.9 Fgf and MAPK signaling are required for localization of Rock2a and MRLC activation.

Figure 1.10 Ras-MAPK and Rock synergize to activate MRLC

Figure 1.11: Ras-MAPK signaling mediates cell-autonomous apical constriction and Rock2a localization.

Chapter 2

Figure 2.1: Ret is required for complete axon extension and is improperly localized in *jip3^{nl7}* mutants.

Figure 2.2: Ret is expressed in pioneer axons during axon extension.

Figure 2.3: Other cargoes do not accumulate in growth cones at 30 hpf in *jip3^{nl7}* mutants.

Figure 2.4: pRet accumulates at the site of distal nerve sever in wildtype larvae, but not in *jip3^{nl7}* mutants.

Figure 2.5: Ret9 is expressed in the pLLg during axon extension.

Figure 2.6: Ret transport during axon extension in wildtypes and *jip3^{nl7}* mutants.

Figure 2.7: Rab5 does not accumulate in growth cones at 30 hpf.

Figure 2.8: Jip-3-Ret9 interaction and Jip-3 domain analysis.

Figure 2.9: Model for Jip3's role as a retrograde adaptor for Ret

Abstract

Functionality of the vertebrate sensory system depends on coordinated development of the signal-transmitting cells called neurons and their sensory organ targets. Neuronal cells undergo dynamic changes in architecture in order to form the unique, polarized structures characteristic of neurons: axons and dendrites. In sensory systems, the sensory structures that neurons innervate also undergo dramatic changes in cell shape in order to form the proper adult sensory organs. Together, these developmental changes in cell characteristics are critical for proper adult sensory perception. However, the complete complement of molecular cues and pathways required for these morphological changes have not been fully elucidated.

During embryonic development, apical constriction drives cell shape changes important for diverse developmental processes, including gastrulation and neural tube closure (Sawyer et al., 2010). This cellular behavior is characterized by the narrowing of the apical domain of an initially columnar cell. Typically, this process is dependent on contraction of an acto-myosin network. However, the extracellular signals that drive this behavior in multiple contexts are not well understood. In this work, we ask how extracellular signals regulate apical constriction during development of the zebrafish posterior lateral line (pLL), a mechanosensory organ system. Formation of the pLL is reliant upon establishment of transient structures called rosettes that are formed through apical constriction. Rosettes will ultimately be deposited along the embryonic trunk and differentiate into mechanosensory organs called neuromasts (NMs). In

this work, we define a novel role for the extracellular signaling molecule Fibroblast Growth Factor (Fgf) in controlling apical constriction through Rho-kinase 2a (*Chapter 1*).

Concurrent with development of pLL mechanosensory organs, afferent axons extend to innervate nascent NMs. The cell bodies of these very long axons reside behind the ear in the posterior lateral line ganglion (pLLg). Proper outgrowth of pLLg axons depends on function of the receptor tyrosine kinase Ret and its ligand GDNF. Here, we show that proper localization of Ret in the growth cones of extending axons is dependent of the scaffolding molecule JNK-interacting protein 3 (Jip3). Using a zebrafish mutant for Jip3, we show that Jip3 is required for proper transport of Ret, and in the absence of Jip3, Ret accumulates in the growth cones and axons fail to completely extend (*Chapter 2*).

A complete understanding of the processes that drive vertebrate organ development is critical for improving treatment of developmental disorders for human patients. Together, the studies presented here reveal how molecular signals drive changes in cell shape. The two models for cell shape change studied here, the neurons and sensory cells of the zebrafish posterior lateral line, are complementary and distinct in terms of the signals required for proper morphogenesis. We show that deregulation of these molecules and signals cause improper formation of sensory organ systems.

Introduction

Modified from: Harding MJ, McCarroll MN, McGraw HF, Nechiporuk AV. Ear and Lateral line Development of Vertebrates: Organization and Development. Encyclopedia of Life Sciences. (2013) *In Press*.

Introduction

Changes in cell morphology during development underlie formation of many organs in biological organisms. Early in development, cell shapes are generally homogeneous, lacking distinct features. As development progresses, these formerly indistinguishable cells undergo changes in morphology and shape, and these changes are critical for the proper development and function of juvenile and adult organ systems. The signals and molecular mediators of these changes are under active investigation.

Sensory perception underlies an organism's ability to navigate its environment and behave properly in response to changes; this ability is critical for survival and reproduction. Sensory information is received and processed by the nervous system, in which cell morphology is particularly diverse. Neurons, the central component of the nervous system, have multiple processes termed axons and dendrites that are necessary for communicating information over distance. In vertebrates, sensory information is detected through multiple organ systems that detect light, sound, touch and other environmental stimuli. These sensory organs include the retina, cochlea and multiple receptors in the dermis. The cells within these organs have distinct morphological features necessary for relay of sensory information. Aquatic vertebrates have an additional sensory system that mediates sensation of water currents, called the lateral line. This sensory organ system promotes behaviors including predator avoidance, schooling, mating and foraging.

The lateral line is composed of mechanosensory organs called neuromasts (NMs) that are arrayed on the surface of the animal. Each NM is composed of approximately 20-30 mechanosensory hair cells, which are morphologically and functionally similar to the hair cells of the vestibular/auditory system (Nicolson, 2005; Whitfield, 2002). These cells have a distinct, teardrop morphology and are innervated by sensory neurons that possess dramatically long axons. During development of the neuronal and sensory components of the lateral line, cells undergo distinct and dynamic rearrangements in morphology, ultimately forming the functional adult lateral line. Because of these rearrangements, the lateral line has emerged as an attractive system to study changes in cell morphology during vertebrate development.

Development of the lateral line has been most carefully studied in the vertebrate model organism zebrafish (*Danio rerio*), as this model system possess advanced molecular tools. In this introduction, I summarize the current understanding of lateral line organization and development.

Function and Features of the Lateral Line

Mechanosensory Hair Cells

Mechanosensitive hair cells are the sensory component in lateral line NMs of aquatic vertebrates, as well as in the ear and vestibular organs. Hair cells convert mechanical stimuli into an electrical response that is transmitted to the nervous system via synaptic connections between hair cells and afferent innervation. The apical domain of hair cells is specialized to respond to the

mechanical stimuli; a single, axonemal kinocilium and multiple rows of variable length actin-filled stereocilia form a staircase-like apical bundle, for which hair cells are aptly named. Adjacent stereocilia are physically joined through lateral links and tip links (Fig. 1). These bundles are extremely sensitive to mechanical deflection by opening and closing ion channels in response to directional deflection.

Mechanically gated channels positioned in the stereocilia allow hair cells to respond to mechanical stimuli. These channels appear to be physically located at the base of the tip link apparatus, as revealed by recent, high-resolution calcium imaging (Beurg et al., 2008). While the identity of this channel has remained elusive, many of the molecules that form the mechanotransduction apparatus have been identified and described. Cadherin 23 and protocadherin 15 interact heterophilically to form the upper and lower portions of the tip link, respectively (Kazmierczak et al., 2007). Tip links are apparently tethered to the mechanotransduction channel.

Deflection of the stereocilia towards the kinocilium causes opening of ion channels, through increased tension on the tip links, resulting in an inward current. This depolarizing potential triggers fusion of synaptic vesicles from a specialized ribbon synapse, releasing the neurotransmitter glutamate at the base of the hair cell (Fig. 1). The release of vesicles is graded, proportional to both the change in potential and degree of bundle deflection. In contrast, bundle deflection in the opposite direction causes relaxation of the tip link and closing of the mechanotransduction channel.

Lateral Line and Neuromast Organization

NM hair cells have basally localized nuclei and apical stereocilia. Stereocilia are arranged in rows of increasing length with a single much longer kinocilium, all of which extend past the skin and are encased in a cupula (Cernuda-Cernuda and García-Fernández, 1996). The stereocilia and kinocilia of hair cells within individual NMs are organized in a pattern of symmetry such that each NM contains two types of cells; half respond to water flow of one direction, and the other half respond to water flow from the opposite direction. Within the lateral line there is a set of NMs that are oriented anterior-posteriorly and another that is oriented dorso-ventrally, allowing the organisms to detect a variety of water movements. Support cells surround the hair cells, providing trophic support and also act as progenitor cells that proliferate to replenish damaged and dead hair cells. Hair cells and support cells are surrounded by mantle cells that may act as slow cycling progenitors (Ma et al., 2008; Raible and Kruse, 2000).

Afferent and efferent innervation of the neuromasts

NMs are innervated by afferent axons extending from the sensory neurons of the lateral line ganglion. These neurons also send projections ipsilaterally to the medial octavo-lateral nucleus of the hindbrain for higher order processing (Raible and Kruse, 2000). Labeling of individual sensory axons in the developing zebrafish lateral line revealed that each NM is innervated by at least two afferent axons that synapse on hair cells of similar orientation (Faucherre et al., 2009). In addition, individual axons synapse on hair cells of multiple, consecutive NMs.

This orientation-specific innervation of hair cells has been suggested to play a crucial role in properly processing the complex information from the multiple NMs across the surface of the animal.

Efferent axons from the hindbrain and hypothalamus also innervate the lateral line system. The efferent system has an inhibitory effect on hair cells mediated in part by acetylcholine and catecholamine depending on the location of the neurons. Together, the afferent and efferent systems coordinate transmission of mechanosensory signals from the lateral line system to the CNS.

Development of the mechanosensory lateral line

Development of the lateral line has been most carefully studied during zebrafish embryonic development. In zebrafish, the lateral line has two components; NMs of the head compose the anterior lateral line (aLL), while the posterior lateral line (pLL) includes NMs of the trunk and body. Recent studies have focused on understanding development of the primary pLL, which begins to form around 20 hours post fertilization (hpf) from the pLL placode, an ectodermal thickening behind the otic vesicle (described below). The caudal portion of the pLL placode migrates toward the tail as an organized group of cells called the pLL primordium (pLLp). The pLLp is a cohort of ~100 cells made up of proliferating progenitor cells and organized epithelial cells that act as proto-NMs. As the pLLp migrates, it deposits proto-NMs every 5-7 somites. Proto-NMs will then differentiate into the hair cells and support cells of the NMs. pLL also deposits a single line of cells, inter-NM cells; these are precursors for additional

NMs that will form during larval development. By 48 hpf, the pLLp has reached the end of the tail, deposited approximately 6 neuromasts along the trunk, and fragmented into a terminal cluster of 2-3 NMs.

Cellular Origin of the pLLp

By 18 hpf, pLL precursors condense into the pLL placode located just caudal to the developing ear. The pLLp is derived from the posterior aspects of this placode, while the anterior portion gives rise to the sensory neurons of the pLL ganglion. pLLp patterning begins before the onset of migration: a first proto-NM, which is structurally a polarized epithelial rosette, appears in the anterior portion of the pLLp at 19 hpf. In the next few hours, rosettes are added to the posterior portion of the pLLp, with migration beginning once two or three rosettes have formed (Nechiporuk and Raible, 2008) at 20 hpf. Early in their course of migration, pLLp cells fuse with a cluster of cells located just caudal to the pLL placode, referred to as separate primordial cells (SPCs). These cells appear to contribute to the leading portion of the pLLp and to terminal NMs (Breau et al., 2012). This cohesive set of cells then migrates towards the tail to form the nascent pLL.

Organization of the posterior lateral line primordium

During migration, the pLLp cells undergo reiterated cycles of NM deposition, cell division and structural rearrangement. The most leading, posterior cells are termed “tip cells;” they demonstrate extensive protrusive

activity of leading processes (Haas and Gilmour, 2006), though their molecular characteristics are not well understood. Other cells in the leading cells region of the pLLp represent the proliferating progenitor cells (Fig. 2B, red cells). The trailing portion of the pLLp is organized into 3-4 rosettes, with each rosette representing a proto-NM (Ghysen and Dambly-Chaudière, 2007) (Fig. 2B). Within rosettes, cells are apically constricted and nuclei are basally displaced (Lecaudey et al., 2008). Constricted apical domains are positioned towards rosette centers, resulting in garlic-bulb shaped structures that will differentiate into hair cell containing NMs. As the pLLp migrates, mature rosettes are deposited from the trailing edge and give rise to mechanosensory neuromasts.

Directional migration

Chemokine signaling coordinates the directional and consistent migration of the pLLp along the trunk midline. The chemokine ligand *sdf1a/cxcl12* is expressed along the horizontal myoseptum, while two chemokine receptors, *cxcr7b* and *cxcr4b* are expressed in the leading and trailing portions of the pLLp, respectively. Disruption of either receptor leads to stalling of pLLp migration, suggesting that both receptors are necessary. In other systems, Cxcr7b acts as a Sdf1a sink, binding ligand without activation of downstream signaling pathways (Boldajipour et al., 2008). If a similar mechanism is present in the pLLp it could account for directional migration of the pLLp, despite homogenous *sdf1a* expression along the trunk midline.

Progenitor cell identity and maintenance

Although the pLLp contains ~100 cells at any given time during its migration, by 48 hpf, the nascent pLL is comprised of ~300 cells (Laguerre et al., 2009), indicating that cellular proliferation is required for pLL organogenesis. The primary source of cellular addition in the pLLp are a population of progenitor cells that reside in the leading, caudal zone (McGraw et al., 2011; Nechiporuk and Raible, 2008) (Fig. 2B, red cells). This region is characterized by high expression of canonical Wnt pathway signaling molecules, such as *lef1* and *axin2* (Aman and Piotrowski, 2008). Multiple studies have shown that pLL formation is extremely sensitive to alterations in Wnt signaling. Over activation of the Wnt pathway leads to excessive proliferation and incomplete migration of the pLLp (Aman and Piotrowski, 2008). Global inhibition of the Wnt/ β -catenin pathway results in severe defects in pLLp migration, patterning and NM deposition due to a dramatic decrease in proliferation and an increase in cell death (Aman et al., 2011; McGraw et al., 2011). In contrast, mutation in the Wnt effector *lef1* ultimately results in pLL truncation and incomplete NM deposition, due to loss of progenitor cell identity but not proliferation (McGraw et al., 2011). Additionally, this disruption in *lef1* may also impact NM deposition rate (Valdivia et al., 2011) (Wnt-dependent NM deposition is discussed below). The difference between global Wnt disruption and the *lef1* mutant phenotype suggests that canonical Wnt signaling has multiple downstream effectors in the pLLp. In support of this, Wnt signaling is required for initiation of FGF signaling (Aman and Piotrowski, 2008), another molecular pathway essential for pLLp patterning

(discussed below). However, the *lef1* mutant shows no changes in *pea3* expression, a direct transcriptional target of FGF pathway (McGraw et al., 2011).

Hair cell precursor specification

FGF signaling is also necessary for formation of hair cell precursors. A small number of cells within each rosette express hair cell-specific transcripts, including *atoh1* and *deltaA*. As rosettes mature, this expression is restricted to fewer cells, a result of classical, notch-delta mediated lateral inhibition (Itoh and Chitnis, 2001). Hair cell precursor specification is FGF-dependent, as loss of FGF results in absence of *atoh1* hair cell precursors in the pLLp (Nechiporuk and Raible, 2008). In contrast, disruption of the Wnt pathway in *lef1* mutants does not alter hair cell precursor specification, though does result in a truncated lateral line (McGraw et al., 2011). Once deposited, an individual hair cell precursor gives rise to multiple HCs of opposing polarity. This is achieved through oriented cell division, coordinated by the planar cell polarity and Notch pathways; daughter cells develop into HCs with opposing apical bundle polarity (López-Schier and Hudspeth, 2006).

Neuromast Deposition

Deposition of neuromasts is regular; a nascent NM is deposited every 5-7 somites along the embryonic trunk. However, the molecular mechanisms that regulate this periodicity are not well understood. Reduction of FGF signaling, chemically or genetically, results in deposition of fewer NMs farther apart along

the trunk (Nechiporuk and Raible, 2008). However, because FGF signaling is also required for formation of rosettes, the NM deposition defect may be secondary. Two specific genes have been implicated in NM deposition, independent of pLLp migration: *Tasctd* is a putative calcium sensor and is highly expressed in trailing pLLp cells just prior to deposition (Villablanca et al., 2006). Similarly, the receptor tyrosine kinase *met* is expressed in the pLLp and reduction of *met* causes pLLp-migration independent NM deposition defects (Haines et al., 2004).

Recently, several groups have suggested a direct link between the rate of proliferation in the pLLp and NM deposition (Aman et al., 2011; Laguerre et al., 2009). Wnt/ β -catenin controlled proliferation in the leading region causes continual addition of cells to the pLLp, resulting in pLLp lengthening and displacement of trailing NMs (Aman et al., 2011). More recently, it has been suggested that Wnt and FGF signaling pathways coordinate NM deposition (Matsuda et al., 2013), through the Lef1 target gene, *dusp6* (negative regulator of Fgf pathway). In the future, it will be interesting to address how these molecular pathways drive the cellular changes required for proper NM deposition.

Rosette Formation and Renewal

NM deposition results in a reiterated “loss” of rosettes from the pLLp. Concurrently, new rosettes are generated rostral to the progenitor domain in the central portion of the pLLp (Nechiporuk and Raible, 2008) (Fig. 2B). Newly generated cells undergo apicobasal polarization, concurrent with alignment of apical domains along midline of the pLLp. In a coordinated manner, their apical

domains constrict giving rise to a nascent rosette (Harding and Nechiporuk, 2012; Lecaudey et al., 2008). As they mature, newly formed rosettes move into the trailing region of the pLLp in a conveyor-belt like fashion.

Rosette renewal in the pLLp is dependent on Fibroblast Growth Factor (FGF) signaling (Lecaudey et al., 2008; Nechiporuk and Raible, 2008). In the absence of FGF signaling, rosettes fail to form and migration of the pLLp stalls. Recently, several complementary studies have revealed the molecular role of FGF signaling in driving rosette renewal. As demonstrated in this dissertation, we have shown that Ras-MAPK signaling is an important intracellular mediator of FGF-dependent rosette formation, activating Rho-kinase dependent Myosin-II activity (Harding and Nechiporuk, 2012). Recently, Ernst et al. showed that activation of the FGF pathway promotes transcription of the scaffolding molecule *Shroom3*, which is required for the apical constriction of newly formed rosettes (Ernst et al., 2012). Together, these studies suggest a model in which FGF-Ras-MAPK signaling causes transcriptional activation of *Shroom3*; in turn, newly generated *Shroom3* recruits Rho-kinase to the apical end of columnar cells, driving activation of myosin-II and subsequent apical constriction (Fig. 2C).

Several groups have suggested that hair cell precursors are responsible for promoting apical constriction and rosette renewal in the leading portion as well as rosette maintenance in the trailing portion (Ernst et al., 2012; Lecaudey et al., 2008). Indeed, there is much evidence that a centrally localized hair cell precursor is likely a source of Fgf ligands in more trailing rosettes (Ernst et al., 2012; Lecaudey et al., 2008). In contrast, FGF3 and 10 are expressed relatively

broadly in the leading rosette renewal region of the pLLp (Nechiporuk and Raible, 2008), encompassing many cells in addition to hair cell precursors. Similarly, we show that the FGF-downstream target MAPK is broadly activated in the rosette-renewal region, indicating that many leading cells both express and respond to FGF (Harding and Nechiporuk, 2012). As many cells in the rosette-forming region of the pLLp are capable of producing and responding to FGF, it is unlikely that hair cell precursors are exclusively responsible for driving rosette renewal. However, in later, more mature rosettes, a single hair cell precursor is likely responsible for maintaining rosette structure through restricted FGF-ligand expression.

LL afferent and efferent axon extension

The afferent neurons that innervate pLL NMs are derived from the pLL placode. These cells that will form the pLL ganglion remain positioned behind the ear during pLLp migration. A subset of these neurons gives rise to pioneer axons, growth cones of which are embedded in the pLLp. These pioneer axons are towed by the pLLp and extend along the migratory route of the pLLp (Gilmour et al., 2004; Metcalfe, 1985) (Fig. 2D). These pioneer axons will eventually innervate terminal cluster NMs. Relative to other pLL neurons, the cells extending pioneer axons differentiate earliest and have a large cell body volume (Pujol-Martí et al., 2012) (Fig. 2A,D).

The association between LL pioneers and the migrating pLLp is dependent on Ret/GDNF signaling. The soluble growth factor GDNF is

expressed in the migrating pLLp, while Ret and its co-receptors Gfra1a and Gfra1b are expressed in the pLL ganglion (Schuster et al., 2010; Shepherd et al., 2004). Combined knockdown of both GDNF and Ret using antisense oligonucleotides causes failure of axon outgrowth without affecting pLLp migration. This evidence suggests that the Ret/GDNF interaction is required for axon extension (Schuster et al., 2010). In this model, pLL pioneers respond to GDNF by binding to and activating Ret, likely positioned on the pioneer axon growth cones. A more detailed analysis of the molecular mechanism is required to fully understand lateral line axon extension. In Chapter 2 of this dissertation, I show that the scaffolding molecule Jip-3 is required for transport of Ret, and this activity is critical for axon extension.

Afferent axons that innervate proximal trunk NMs are termed “follower” axons (Fig. 2D, light green cells). As their name suggest, these axons extend later than the pLLp-embedded pioneer axons (Fig. 2D, dark green cells) (Gompel et al., 2001). Additionally, the cell bodies of these axons have smaller volume (Pujol-Martí et al., 2012) and the growth cones are less elaborated in morphology (Gompel et al., 2001). The molecular mechanisms that drive extension of these later-extending axons are not clear at this time. Finally, efferent axon extension is suggested to be independent of pLLp migration, and instead may use the extending afferent axons for guidance (Sapède et al., 2005).

Conclusion

This introduction summarizes the current understanding of lateral line development and function. In individual chapters, independent introductions are

arranged to more completely introduce the appropriate background for each project and set of experiments that follow.

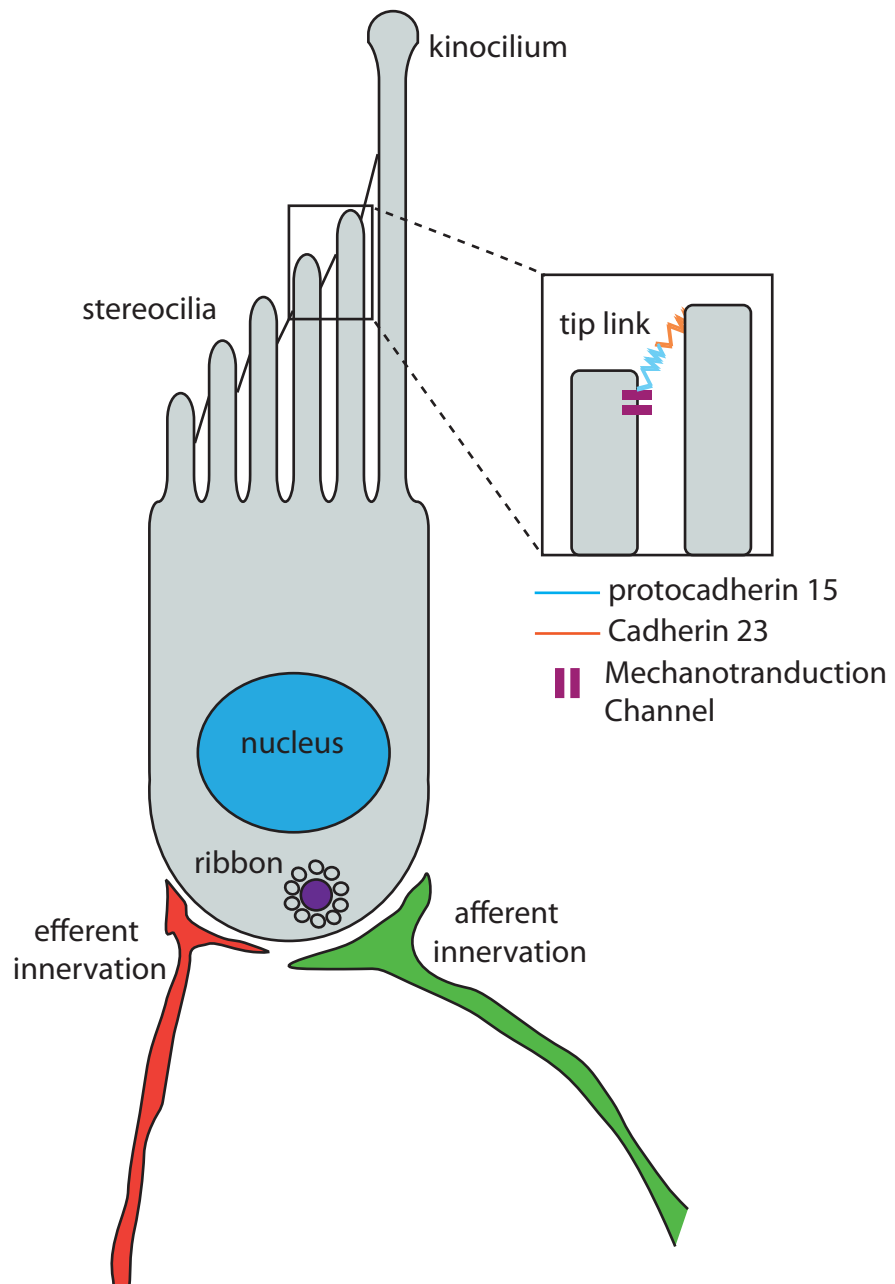


Figure 1. Mechanosensory hair cells and development of the posterior lateral line. (A) Schematic showing general features of the hair cell. The apical end includes stereocilia and kinocilium-containing hair bundle, tip links and mechanotransduction channel. Basal features include the ribbon synapse, afferent and efferent innervation.

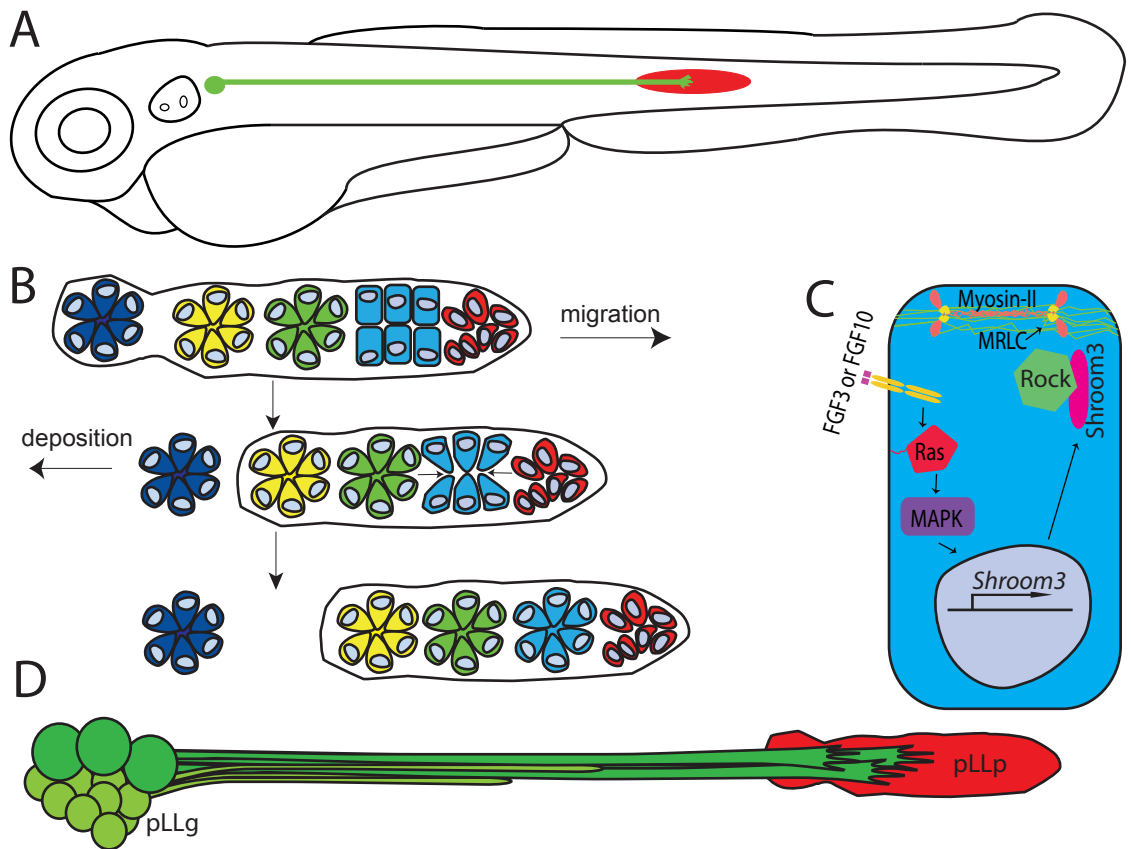


Figure 2: Development of the posterior lateral line. (A) 30hpf zebrafish embryo. PLLg is positioned behind the ear, with pLLp (red) migrating down the trunk. (B) Rosette renewal in the pLLp. Leading region progenitors (red) give rise to columnar daughter cells (blue), which constrict apically to give rise to a nascent rosette. Mature rosettes are deposited at the trailing part of the pLLp. (C) Model of apical constriction in the leading portion of the pLLp. FGF activates the Ras-MAPK pathway, which likely transcriptionally activates shroom3. Shroom3 anchors Rho-kinase (Rock) in the apical domain of the cell, activating the acto-myosin cytoskeleton. (D) Lateral line axon extension. Pioneer axons (dark green) extend with the primordium. Follower axons (light green) extend later.

Chapter 1: FgfR-Ras-MAPK signaling is required for apical constriction via apical positioning of Rho-kinase during mechanosensory organ formation.

Modified from: Harding MJ, Nechiporuk AV. FGF-Ras-MAPK signaling controls apical constriction via apical positioning of Rho kinase during mechanosensory organ formation. *Development*. (2012) Sep;139(17):3130-5.

Abstract:

Many morphogenetic movements during development require formation of transient intermediate cellular arrangements called rosettes. Within rosettes, cells are polarized with apical ends constricted towards the rosette center and nuclei are basally displaced. While the polarity and cytoskeletal machinery establishing these structures has been extensively studied, extracellular cues and intracellular signaling cascades promoting formation of these structures are not well understood. We asked how extracellular Fibroblast Growth Factor (Fgf) signals regulate rosette formation in the zebrafish posterior lateral line primordium (pLLp). The pLLp is a group of ~100 cells that migrates along the trunk of the zebrafish during embryonic development, forming the lateral line mechanosensory system. During migration, the pLLp deposits rosettes from the trailing edge, while cells are polarized and incorporated into nascent rosettes in the leading region. Fgf signaling was previously shown to be critical for rosette formation in the pLLp. We demonstrate that activation of Fgf receptor (FgfR) induces intracellular Ras-MAPK to drive apical constriction and rosette formation in the pLLp. Inhibiting FgfR-Ras-MAPK leads to a loss of apically localized Rho-kinase (Rock) 2a, which results in failed acto-myosin cytoskeleton activation. Using mosaic analyses, we show that a cell-autonomous Ras-MAPK signal drives apical constriction and Rock2a localization. Based on these data, we propose a model where activated FgfR signals through Ras-MAPK to induce apical localization of Rock2a in a cell-autonomous manner, activating the acto-myosin network to promote apical constriction and rosette formation in the pLLp.

This previously unrecognized mechanism comprises a novel cellular strategy for driving cell shape changes.

Introduction:

Apical constriction is a cell shape transition that results from narrowing of the apical side of an initially columnar cell. In multiple species, apical constriction drives tissue reorganization important for diverse developmental processes, including gastrulation and neural tube closure (Sawyer et al. 2010). This cellular behavior is typically dependent on contraction of an apical acto-myosin network, composed of non-muscle Myosin (Myosin-II) and an apical meshwork of filamentous actin (F-actin). To form this network, an apical domain is initially established through activity of the Par proteins (A. Suzuki and Ohno 2006) and apical localization of the microtubule organizer γ -tubulin. Subsequently, components of the cytoskeleton, including F-actin, Myosin-II and adherens junctions, accumulate in the apical domain. Finally, the molecular motor Myosin-II is activated by phosphorylation of Myosin Regulatory Light Chain (MRLC), relieving auto-inhibition and driving constriction (Reviewed in Sawyer et al., 2010 and Somlyo and Somlyo, 2003). Activation of MRLC is critical for activity of myosin and is mediated by multiple kinases, including Rho-kinase (Rock; (Vicente-Manzanares et al. 2009). While the cytoskeletal network driving constriction is fairly well understood, how extracellular cues regulate this process in the context of tissue development is largely unknown. Here, we ask how extracellular signals regulate apical constriction during rosette formation in the zebrafish posterior lateral line primordium (pLLp).

During lateral line development, a subset of cells in the pLLp are organized into rosettes (Ghysen and Dambly-Chaudière 2007); within rosettes, cells are apically constricted, with basally displaced nuclei (Lecaudey et al. 2008). As the migrating pLLp deposits mature rosettes from the trailing edge that give rise to mechanosensory neuromasts, new cells are generated, polarized and assembled into nascent rosettes in the leading edge (Nechiporuk and Raible 2008). We and others have previously demonstrated that rosette renewal in the pLLp is dependent on Fibroblast Growth Factor (Fgf) signaling (Lecaudey et al. 2008; Nechiporuk and Raible 2008). However, the mechanism by which extracellular Fgf is interpreted intracellularly to control cell shape is not understood.

Fgfs are secreted molecules that promote diverse cellular processes including survival and fate specification. Upon binding to transmembrane receptors, Fgfs activate multiple intracellular cascades, including the Ras-MAP kinase (ERK) pathway (Tsang and Dawid 2004). Ras-MAPK signaling mediates multiple processes ranging from transcription to cytoskeletal remodeling (Tsang and Dawid 2004). However, whether Ras-MAPK mediates Fgf signaling and cell shape changes in the pLLp is unknown.

Here, We show that the Ras-MAPK pathway is activated in the pLLp in an Fgf-dependent manner, and that FgfR-Ras-MAPK signaling is required cell-autonomously for apical positioning of Rho-kinase and apical constriction, two necessary processes for rosette formation. This previously unrecognized

mechanism is critical for proper pLLp development, and may reveal a novel cellular strategy for driving cell shape changes.

Materials and Methods

Fish strains, heat-shock, pharmacological treatments and live imaging

Adult zebrafish were maintained under standard conditions (Westerfield 1995). The pLLp was visualized using *Tg(-8.0claudinB:lynEGFP)^{zf106}* (Haas and Gilmour 2006), referred to here as *claudinB:EGFP*. Ras signaling was conditionally inhibited using *Tg(hsp70l:dnHRAS,cryaa:EGFP)^{pd7}* (also called *hsp70:dn-Ras*) embryos (Lee et al. 2009) heat-shocked at 28 hpf for 40 minutes at 38°C, unless indicated. Inhibitors were diluted in embryo medium with 1% DMSO and used at the following concentrations, unless indicated: 100 µM SU5402 (Calbiochem), 7µM PD0325901 (Stemgent), 50 µM Blebbistatin (Cayman Chemical) and 50 µM Rockout (Calbiochem). Live imaging was performed as described (Nechiporuk and Raible 2008).

Plasmids and Injections

Par3-EGFP plasmid (Von Trotha, Campos-Ortega, and Reugels 2006) was modified to express Par3-TagRFP fusion. *par3-TagRFP* mRNA was synthesized using mMessage Machine (Life Technologies) and microinjected at 500 pg/embryo.

Immunolabeling and in situ hybridization

Immunolabeling was performed following established protocols (Ungos, Karlstrom, and Raible 2003), with the following exceptions: embryos stained with anti-Rock2a and anti-pMAPK were fixed in Glyo-Fixx (Thermo Scientific) and embryos stained with anti-pMRLC were fixed in Bouin's fixative (Ortiz-Hidalgo 1992). Antibodies used: rabbit anti-GFP (1:1000; Invitrogen), mouse anti-GFP (1:1000; Roche), rabbit anti-pMAPK (1:50; Cell Signaling), rabbit anti-Rock2a (1:50; Anaspec), rabbit anti-pMRLC (1:20; Cell Signaling), rabbit anti- γ -tubulin (1:1000; Sigma), rabbit anti-Myosin-IIA (1:500; Sigma), Alexa Fluor-568 phalloidin (1:500; Invitrogen). In situ hybridization was performed as described (Andermann, Ungos, and Raible 2002). Digoxigenin-labeled antisense RNA probes were generated for the following: *fgfr1* (Scholpp et al. 2004), *pea3* (Raible and Brand 2001, 3), and *fgf10a* (Grandel, Draper, and Schulte-Merker 2000). Fluorescently-labeled embryos were imaged using an FV1000 confocal (Olympus). Images were processed in ImageJ (Abramoff 2004); brightness and contrast were adjusted in Adobe Photoshop.

Cell shape and fluorescence intensity analysis

Three-dimensional reconstructions were generated from images of *claudinB:EGFP* pLLp using Imaris software (Bitplane). Apical constriction indexes (ACI) were generated from manually collected measurements. Measurements were taken from the surface of each cell oriented toward the midline. Apical width measurements were made 1 μ m below the apical surface. Height measurements

represent a straight line between the apical and basal surface. Rock2a apical intensity was measured from the average fluorescence intensity in the apical domain (apical 1/3 of cell) compared to the rest of the cell (basal 2/3).

Transplantation Experiments

Transplantation experiments were carried out as previously described (Nechiporuk and Raible 2008). Host embryos expressed *claudinB:EGFP*, while donor cells contained rhodamine-dextran (Invitrogen). Chimeric embryos were collected at 28 hpf and heat-shocked as described above.

Statistical Analysis

We used JMP (SAS Inc.) to perform one-way ANOVA, Wilcoxon and Tukey-Kramer post-hoc tests. Student's *t*-tests were performed in Microsoft Excel. Data are presented as mean \pm SEM.

Results

Rosette formation is dependent on the FgfR-Ras-MAPK signaling cascade.

To address how Fgf signals are intracellularly interpreted in the pLLp, we tested whether the MAP kinase (MAPK) signaling pathway, a common mediator of Fgf signaling, was active in the pLLp. Activation of the MAPK signaling cascade, detected via phosphorylated MAPK (pMAPK) immunostaining, was observed in pLLp cells and surrounding tissues (Fig. 1.1A). While MAPK

expression pattern was somewhat variable, the majority of cells with high levels of pMAPK were positioned in existing rosettes and in the region where rosettes form (Fig. 1.1A). In the leading-most, progenitor pool of cells of the pLLp (McGraw et al. 2011) pMAPK was not detectable. Blocking Fgf receptor (FgfR) signaling with the chemical inhibitor SU5402 (Mohammadi et al. 1997) resulted in pMAPK loss, indicating that activity of FgfR is required for MAPK cascade activation (Fig. 1.1B). Consistent with previous observations (Lecaudey et al. 2008; Nechiporuk and Raible 2008), inhibiting FgfR activity also interfered with rosette formation in the leading zone (Fig. 1.1A,B, yellow bracket). Blocking Ras-MAPK signaling using *hsp70:dn-Ras* transgenics or the MAPK kinase (MAPKK) inhibitor PD0325901 resulted in loss of the pMAPK signal and a failure of leading rosette formation, phenotypes similar to those observed following FgfR inhibition (Fig. 1.1C,D). Additionally, prolonged treatment with PD0325901 caused a progressive expansion of the rosette-free region (data not shown). We thus conclude that FgfR-Ras-MAPK signaling is necessary for MAPK activation, which is in turn required for rosette formation.

Similar to FgfR inhibition, inhibiting MAPKK squelched Fgf target gene expression (*fgfr1* and *pea3*), suggesting that MAPK mediates Fgf-dependent patterning in the pLLp (Fig. 1.2; Nechiporuk and Raible, 2008). Combinatorial treatment with suboptimal doses of FgfR and MAPKK inhibitors between 30 and 48 hpf caused pLLp migration arrest, implying that Fgf and MAPK function in the same molecular pathway (Fig. 1.3). In addition, combinatorial treatment with suboptimal induction of *hsp70:dnRas* in combination with suboptimal PD0325901

treatment also caused migration arrest (Fig. 1.3). Together, these data show that the Ras-MAPK signaling cascade is the intracellular transducer for FgfR signaling in the pLLp.

The FgfR-Ras-MAPK signaling cascade is required for apical constriction in leading pLLp cells.

Apical constriction has been suggested to underlie pLLp rosette formation (Hava et al. 2009; Chitnis, Nogare, and Matsuda 2012). Cell shape analysis during live-imaging of rosette formation revealed that over the course of one hour, columnar cells become apically constricted as nascent rosettes form (Fig. 1.1E-G), confirming that apical constriction promotes rosette formation.

Because blocking FgfR-Ras-MAPK signaling caused a failure of leading rosette formation, we asked whether FgfR-Ras-MAPK inhibition disrupted apical constriction. We limited our analyses to the leading 30 pLLp cells, as our live imaging indicated that this population gives rise to new rosettes. We measured apical constriction indices (ACIs; ratios of lateral height to apical width) of pLLp cells following 2 hours of FgfR, Ras, or MAPKK inhibition, and compared them to DMSO-treated controls. Control cells had a wide range of ACIs (Fig. 1.1H), reflecting the diverse variety of cell shapes. Cells become more constricted as they moved away from the leading edge, likely incorporated into nascent rosettes (Fig. 1.4A,E). In contrast, the ACIs of treated embryos were smaller, corresponding with failure in apical constriction (Fig. 1.1H; Fig. 1.4B-E). From

these data, we conclude that FgfR-Ras-MAPK signaling is required for apical constriction.

FgfR-Ras-MAPK is not required for subcellular distribution of apical polarity and cytoskeletal components

Analyses in other models have shown that apical polarity establishment and acto-myosin network assembly are important for apical constriction (Sawyer et al. 2010). Because FgfR-Ras-MAPK signaling underlies apical constriction in the pLLp, we asked if MAPK activation modulates localization of polarity molecules (e.g., Par3 and γ -tubulin) or cytoskeletal molecules (e.g., Cadherin-2, F-actin and Myosin-II). To test this, we first analyzed how these molecules are polarized in cells of the rosette-forming region of the pLLp. We found that Par3 and γ -tubulin were apically localized in the leading cells, caudal to the first rosette, demonstrating that cells are polarized prior to apical constriction and rosette formation (Fig. 1.5A-H). Cadherin-2, F-actin and Myosin-II were also localized to apical domains, slightly more rostral relative to the polarity markers (Fig. 1.5I-T). Inhibiting FgfR or MAPKK did not disrupt apical localization of these polarity components (Fig. 1.5A-H), or cytoskeletal components following inhibition of FgfR or MAPKK was unchanged (Fig. 1.5I-T). These data indicate that FgfR-Ras-MAPK signaling is not required for the localization or assembly of cytoskeletal polarity machinery in the pLLp.

Myosin-II is required for rosette formation in the pLLp, but not HC precursor specification

Although Fgf-Ras-MAPK signaling had no impact on localization of cytoskeletal or polarity components, we asked whether Fgf signaling might be involved in Myosin-II activation. We treated embryos with the Myosin-II inhibitor Blebbistatin for 3 hours, beginning at 27 hpf. We observed a failure in rosette formation, leading to eventual stalling of the pLLp and failure in NM deposition, similar to the Fgf-Ras-MAPK inhibition phenotypes. This suggests that Fgf-Ras-MAPK may control rosette formation by activation of Myosin-II (Fig. 1.6).

Rho-kinase is required for apical constriction and activation of MRLC

In order for Myosin-II to generate force, it must be activated through MRLC phosphorylation (Vicente-Manzanares et al. 2009). Because Rho-kinase (Rock) is known to phosphorylate MRLC in other contexts (Ishiuchi and Takeichi 2011; Plageman et al. 2011), we asked whether Rho-kinase was required for Myosin activation during rosette formation in the pLLp. We treated embryos with the Rho-kinase inhibitor Rockout (Weiser, Pyati, and Kimelman 2007) for 2 hours beginning at 28 hpf, and assayed constriction and MRLC phosphorylation. We observed apical constriction failures in leading-edge cells following Rockout treatment (Fig. 1.7A-E). Rock inhibition also resulted in failure of MRLC phosphorylation in the leading edge (Fig. 1.7F-H). From these data, we conclude that Rock activity is required to activate MRLC in the pLLp and drive apical constriction during rosette formation.

FgfR-Ras-MAPK is required for subcellular distribution of Rho-kinase 2a

Next, we asked whether FgfR-Ras-MAPK regulated subcellular localization of Rock during pLLp apical constriction. We focused on Rock2a, as Rock2a is the predominant Rho-kinase in neuronal tissues (Amano, Nakayama, and Kaibuchi 2010) and is expressed in the pLLp (Fig. 1.8). A second isoform, Rock2b, did not appear to be expressed in the pLLp (Wang et al. 2011). In control embryos, Rock2a was apically localized in leading cells. However, following FgfR or MAPKK inhibition, Rock2a failed to segregate apically and appeared dispersed throughout the cell (Fig. 1.9A-C). MAPK did not regulate Rock2a transcription, as inhibition of MAPKK did not alter *rock2a* expression (Fig. 1.8). As Rock was required for phosphorylation of MRLC, we asked whether FgfR-Ras-MAPK activity was also necessary for MRLC phosphorylation. Indeed, pMRLC was lost from leading pLLp cells in embryos treated with FgfR or MAPKK inhibitors (Fig. 1.9D-F). This implies that proper Rock2a localization is required for the activation of MRLC. Interestingly, loss of apical Rock2a and pMRLC activation was unchanged in trailing rosettes following FgfR-Ras-MAPK inhibition, indicating that this pathway is required for the initiation of Rock2a apical positioning, but not its maintenance. Finally, combining suboptimal inhibition of Ras-MAPK signaling with suboptimal inhibition of Rockout resulted in a failure of MRLC activation in the leading pLLp cells (Fig. 1.10), suggesting that Ras-MAPK and Rock2a act in the same pathway.

Ras-MAPK signaling is required cell-autonomously to localize Rock2a and drive apical constriction

We next asked whether individual pLLp cells lacking Ras-MAPK signaling were capable of apically constricting in the context of wildtype neighbors. To address this question, we generated mosaic embryos that contained a small number of *hsp70:dn-Ras* or wildtype (control) donor cells. Mosaic embryos were heat-shocked at 28 hpf to inhibit Ras activity; pMAPK expression and apical constriction were assayed at 30 hpf. As expected, induction of *dn-Ras* in donor cells resulted in loss of pMAPK (Fig. 1.11A,B). Reconstructed cell shapes from before and after heat-shock showed that wildtype cells constricted over the 2-hour period (Fig. 1.11C). In contrast, average ACIs of Ras-deficient cells did not change, indicating constriction failures (Fig. 1.11D-D',E). Loss of Ras-MAPK activity also corresponded to cell-autonomous loss of apical Rock2a in *dn-Ras* cells (Fig 11.H,I). However, this loss had no obvious effects on the overall distribution of Rock2a (Fig. 1.11F,F',G,G'). Our data show that individual cells constrict in response to intracellular Ras-MAPK initiating apical accumulation of Rock2a, and not as a result of neighbor interactions.

Discussion

Together, our data demonstrate a novel pathway by which extracellular cues direct changes in the cellular cytoskeleton that drive changes in cell morphology, during organogenesis. We show that in the context of the pLLp, activity of the FgfR and its downstream effector Ras is required for activation of MAPK. We

also show that MAPK is required for apical constriction, which in turn drives rosette formation. Finally, we demonstrate that FgfR-Ras-MAPK signaling drives activation of an apical acto-myosin network by apical positioning of Rho-kinase 2a.

Our observations reveal a novel role for FgfR signaling during morphogenesis and might represent a more general strategy for controlling apical constriction. Fgf signaling has previously been implicated in apical constriction via activation of basally-localized Myosin-II during inner ear morphogenesis (Sai and Ladher 2008). However, our data provide the first example that FgfR signaling, through the Ras-MAPK pathway, regulates localization of Rock without affecting other polarity or cytoskeletal components. When combined with Fgf's role in pLLp hair cell specification (Nechiporuk and Raible 2008), this model elucidates the well coordinated manner in which Fgf is required independently for both morphogenesis and patterning of the pLLp.

Regulation of Rock2 localization

An intriguing question raised by this work is how FgfR-Ras-MAPK acts to regulate apical localization of Rock2a. While Rock does not contain a consensus sequence for MAPK phosphorylation, MAPK has previously been implicated in Rock activation via phosphorylation and suppression of the RhoGAP p190A and subsequent promotion of RhoA/Rock activity (Pullikuth and Catling 2010). Another possibility is that, Ras-MAPK signaling might activate transcription of *shroom3*, a scaffolding molecule that can anchor Rock and promote apical Rock

localization (Nishimura and Takeichi 2008). Shortly after publication of the manuscript summarized in this chapter (Harding and Nechiporuk 2012), another study was published showing that Fgf controls transcription of *shroom3*, and that Shroom3 is required for rosette formation (Ernst et al. 2012). This study both supports and complements the findings presented here. Together, our data and this more recent study suggest a model in which Fgf signaling activates Ras-MAPK and in turn upregulates transcription of *Shroom3* (see model in Introduction, Fig. 1C). Newly generated Shroom3 might then recruit Rock2a to the apical cortex of the cell, locally activating the apical acto-myosin network and driving the apical constriction that underlies rosette formation. Further work is needed to test this model.

How is the acto-myosin network assembled?

Whereas FgfR-Ras-MAPK signaling is required for activation of the acto-myosin network, how the acto-myosin network is initially assembled in the leading pLLp cells remains unclear. Cytoskeletal components assemble apically in columnar pLLp cells prior to apical constriction (Fig. 1.5). In the future, it will be interesting to determine which signaling pathways are important in assembly of this network, and how this assembly is coordinated toward the pLLp midline. Wnt signaling is critical for identity and maintenance of the most leading pLLp cells (McGraw et al. 2011; Aman, Nguyen, and Piotrowski 2011; Aman and Piotrowski 2008); perhaps Wnt is also important in formation of the apical cytoskeleton, prior to activation of Fgf signaling required for apical constriction.

Fgf signaling has multiple roles during pLLp patterning

Interestingly, the roles of Fgf in hair cell specification and rosette formation seem to be at least partially independent. While Fgf, Ras and MAPK activity are all required for both induction of hair cell precursor specification (assayed by expression of *atoh1a*) and rosette formation, inhibition of the Myosin-II using the inhibitor Blebbistatin blocks only rosette formation, but not induction of *atoh1a* expression (data not shown). If *Shroom3* is indeed the Fgf-Ras-MAPK-dependent transcriptional target required for rosette formation, hair cell precursor specific genes may be directly or indirectly controlled by Fgf-Ras-MAPK signaling as well. This potential coupling of rosette formation and hair cell precursor induction suggests an elegant model in which transcriptional activation via a single upstream signaling cascade can coordinate multiple downstream effects.

Fgf regulation of rosette formation

One outstanding question raised by this study is: how are apically constricted cells coordinated to form a rosette? While leading cells appear to constrict in a coordinated manner with respect to timing, how is this timing coordinated and biased towards the center of the newly forming rosette? In other systems, it has been suggested that apically constricted cells are physically connected and coordinate through apical adherens junctions in the “purse-string” model (Bement, Forscher, and Mooseker 1993). The existence of such a network in pLLp rosette-forming cells might explain the coordinated constriction of cells within the presumptive rosette. The center-bias of rosette formation has

previously been suggested to rely on secretion of Fgf from a single, *fgf3/10* expressing cell, localized centrally to the rosette-forming cell population (Lecaudey et al. 2008; Ernst et al. 2012). However, as previously demonstrated, Fgf ligands are broadly expressed in the leading portion of the pLLp (Nechiporuk and Raible 2008), though this expression is restricted to a single cell in more mature rosettes. Therefore, although a centrally localized Fgf-expressing cell might maintain rosette integrity as rosettes mature, this model cannot account for the center-biased formation of rosettes. Instead, we propose that the coordinated apical constriction of cells might physically drive formation of a rosette center simply by the properties of the mechanical changes in the tissue morphology; for example, the coordinated apical constriction of cells in the neural tube cause formation of a symmetrical tube with a distinct center point (M. Suzuki, Morita, and Ueno 2012). Perhaps the physical changes associated with coordinated apical constriction inherently drive formation of a central point.

Conclusion

In this study, we have exploited the unique characteristics of the zebrafish pLLp to study the progressive steps required for apical constriction. We have identified a critical signaling pathway, FgfR-Ras-MAPK, which is specifically required for the activation, but not assembly, of the apical cytoskeleton, through the localization and activation of Rho-kinase. A detailed understanding of the

molecular steps necessary for development cell shape changes is critical for a complete understanding of organ formation during development.

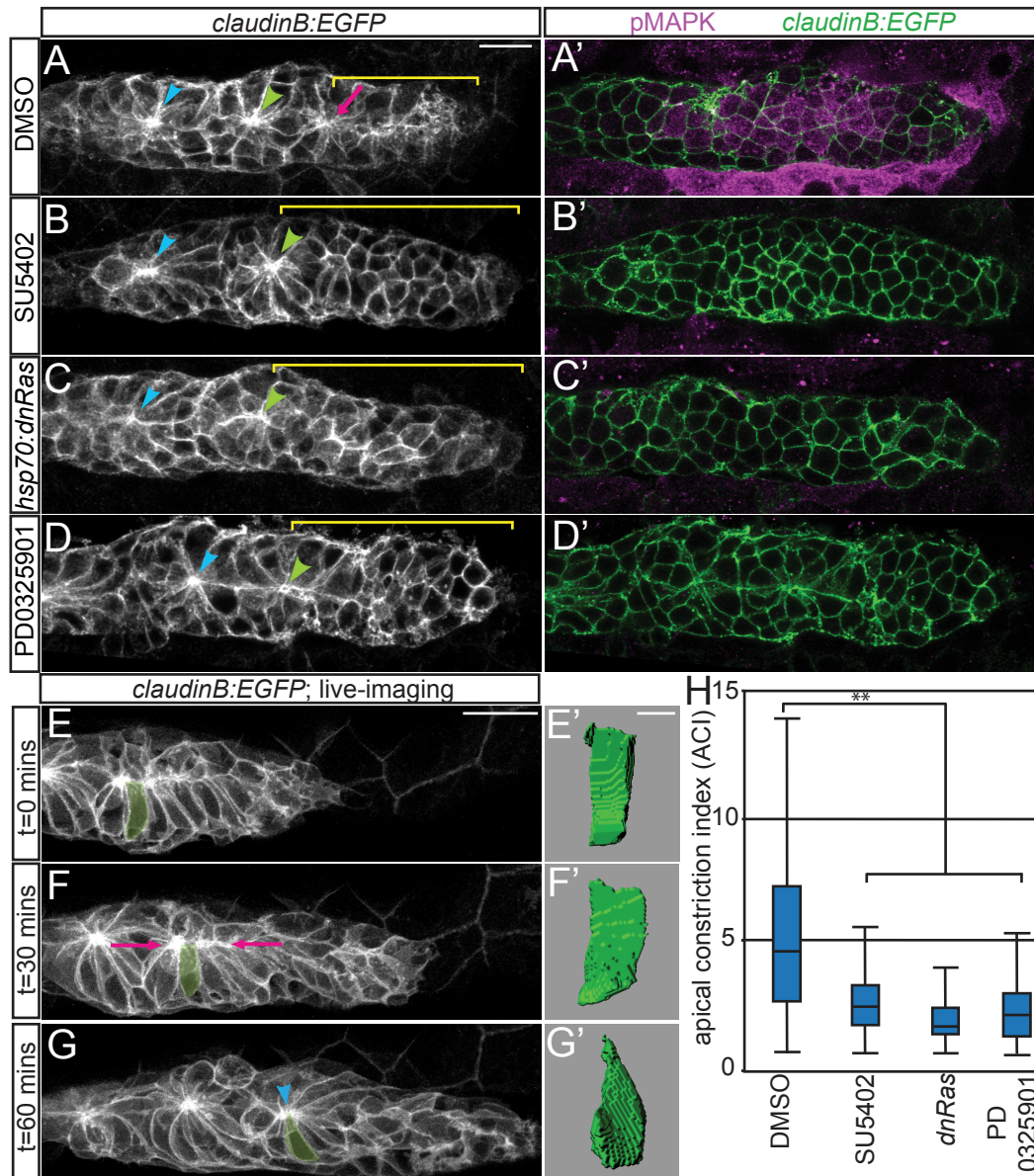


Figure 1.1: Fgf-Ras-MAPK signaling in the pLLp is required for rosette formation. (A-D) Confocal projections showing rosette formation in DMSO-control, FgfR, Ras, and MAPKK inhibited *claudinB:EGFP* embryos at 30 hpf. Arrowheads indicate centers of rosettes. Pink arrow indicates nascent rosette. (A'-D') pMAPK expression in single planes from projections in (A-D). FgfR (B') and MAPKK (D') inhibition with 100 μ M SU5402 and 7 μ M PD0325901, respectively, from 28-30 hpf. Ras inhibition (C') via *hsp70:dn-Ras* at 28 hpf; embryos were fixed 2 hours following heat-shock. (E-G) Stills from time-lapse of pLLp in wild-type *claudinB:EGFP* embryo. (F) Cells align apical ends along the midline (pink arrows). (G) Center of the nascent rosette (arrowhead). (E'-G') Three-dimensional reconstructions of the highlighted cell in (E-G). (H) ACIs for embryos treated with DMSO, SU5402, PD0325901 or following induction of *hsp70:dn-Ras* (n=90 cells from 3 embryos/condition; **p<0.0001, Wilcoxon test). Scale bar=20 μ m in (A-C) and 4 μ m in (E-G).

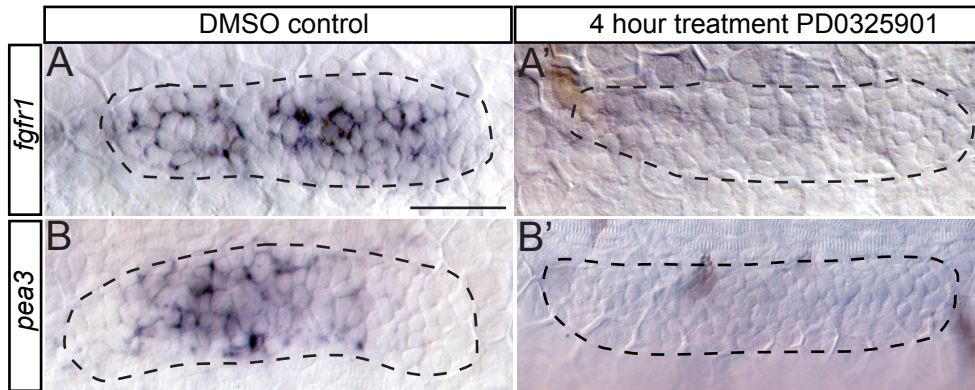


Figure 1.2: Inhibition of MAPKK phenocopies loss of FgfR signaling.
 (A-B) Inhibition of MAPKK with the pharmacological inhibitor PD0325901 between 28 and 32 hpf resulted in a loss of the *fgfr1* (A,A') and *pea3* (B,B') transcripts, compared to DMSO-treated controls (A-B). Scale bar=30 μ m.

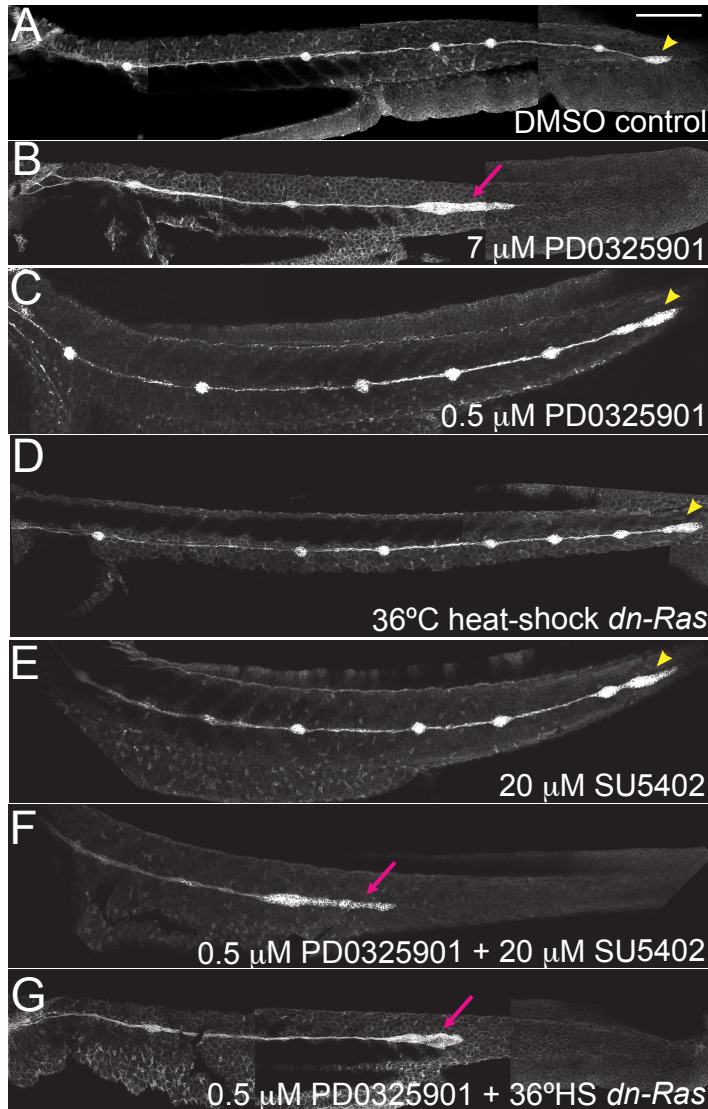


Figure 1.3: FgfR, Ras and MAPK synergize during formation of the posterolateral line. (A-G) Activity of FgfR, Ras or MAPKK were modulated in claudinB:EGFP embryos using pharmacological inhibitors (SU5402 and PD0325901) or expression of a dominant-negative transgene hsp70:dn-Ras between 30 and 48 hpf. (A) In 48-hour old DMSO-treated controls, embryos have deposited 5-6 neuromasts (NMs) along the trunk, and the pLLp has reached the end of the tail to form the terminal cluster of neuromasts. (B) Treatment with optimal dose of PD0325901 (7 μ M) caused a failure of distal neuromasts deposition and a stalling of the pLLp. (C) A suboptimal dose of MAPKK-inhibitor PD0325901 (0.5 μ M) did not affect neuromast deposition or pLLp migration. (D-E) Suboptimal inhibition of Ras (36°C heat-shock of hsp70:dnRas) or FgfR (20 μ M SU5402) did not affect neuromast deposition or pLLp migration. (F-G) Combining suboptimal PD0325901-treatment with suboptimal SU5402-treatment or suboptimal heat-shock of hsp70:dnRas resulted in stalling of the pLLp and failed neuromast deposition. Scale bar=200 μ m.

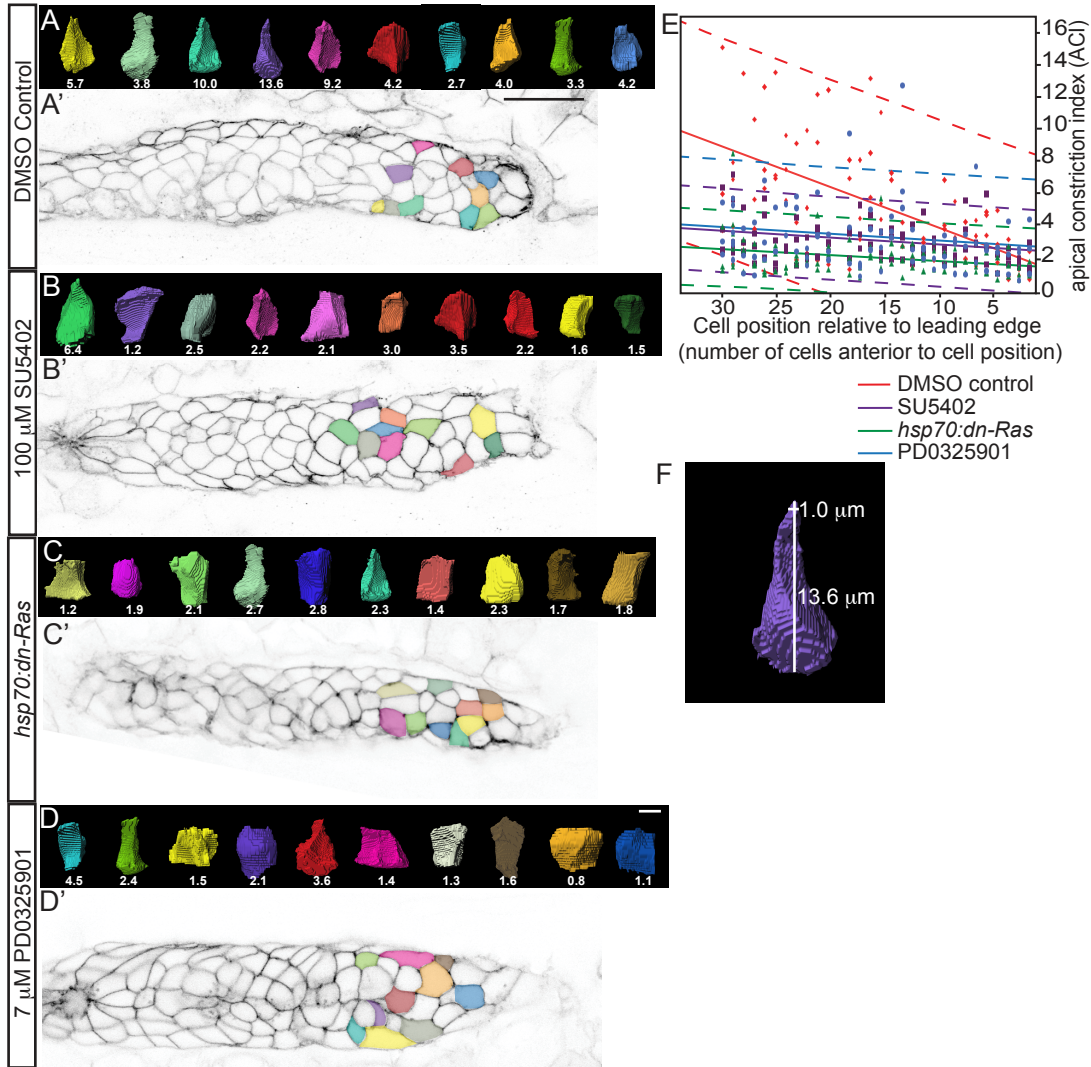


Figure 1.4: FgfR-Ras-MAPK signaling is required for apical constriction.

(A-D) (A) Representative 3-dimensional reconstructions from the leading edge of a DMSO-treated embryo. (A'-D') Single z-slice from confocal stack used to generate 3-dimensional views in (A-D) Color of 3-D reconstruction in (A-D) corresponds to position of cell in (A'-D'); cells selected at random). Numbers below cells indicate measured ACI for each cell. (B-D) 3-D reconstructions from embryos treated with 100 μ M SU5402 or 7 μ M PD0325901 from 28-30 hpf (B and D), or 2 hours following heat-shock induction of *dn-Ras* (C). (E) ACI for the leading 30 cells was measured in 6 embryos per condition (n=180 cells total) and plotted according to absolute number of pLLp cells more anterior than position of measured cell; Position of cell was determined by counting the number of anterior pLLp cells. In control, note that cells have higher ACIs further from the leading edge, consistent with live imaging data that showed cells constricting as the rosettes mature. When FgfR, Ras, or MAPKK were inhibited, cells failed to constrict, resulting in smaller ACIs. Dotted lines indicate 95% confidence interval. (F) Schematic showing measurements technique. Apical width measurements were made 1 μ m below the apical surface, and lateral height was measured from the apical to basal surface.

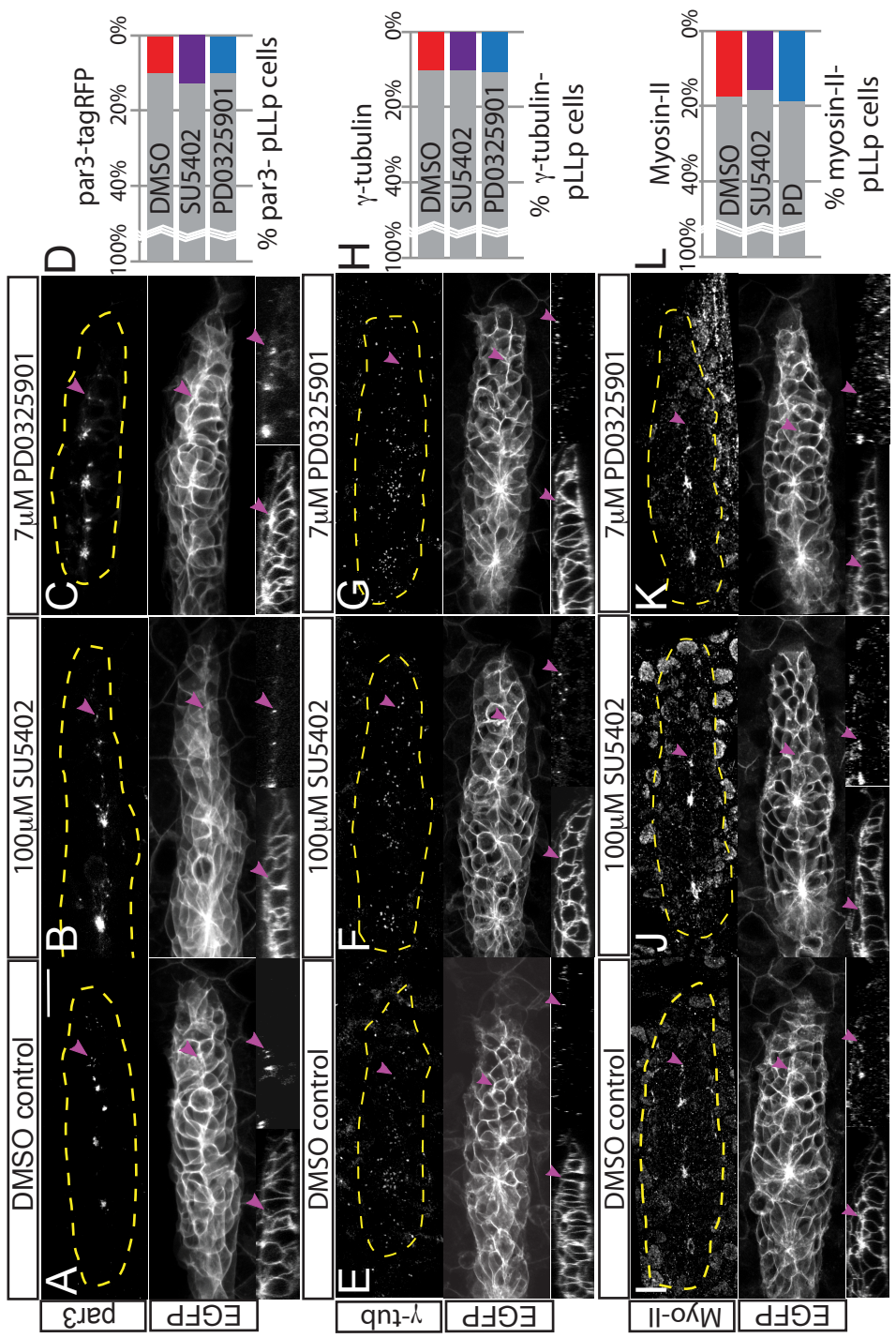


Figure 1.5: Fgfr-Ras-MAPK signaling does not disrupt localization of polarity molecules or the acto-myosin cytoskeleton. (A-L) Analyses of polarity and cytoskeletal recruitment in the pLLp.

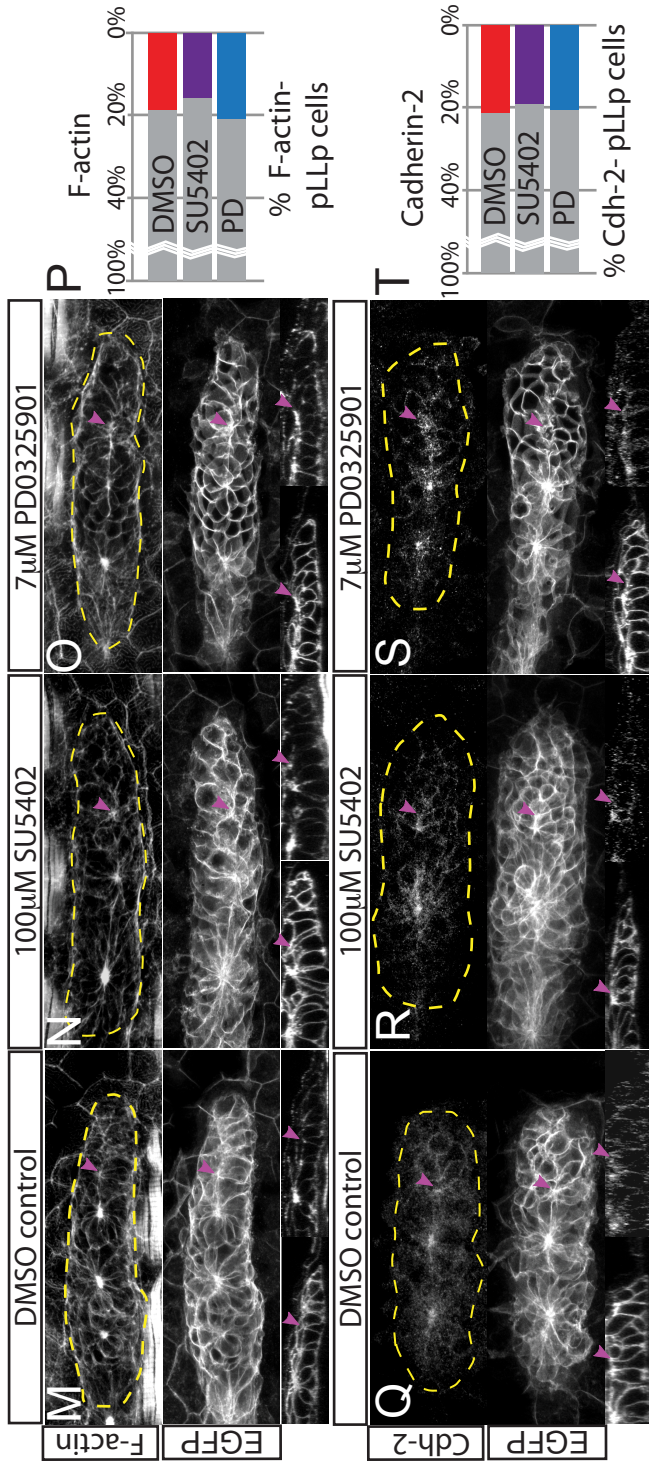


Figure 1.5: FgfR-Ras-MAPK signaling does not disrupt localization of polarity molecules or the actomyosin cytoskeleton (continued). Analyses of polarity and cytoskeletal recruitment in the pLLp. (A-C) Par3 localization was examined by overexpression of par3-TagRFP. Immunohistochemistry was used to examine localization of (E-G) γ -tubulin, (I-K) Myosin-II, (M-O) F-actin and (Q-S) Cadherin-2. Each panel shows indicated molecule (top), claudinB:EGFP (middle) and sagittal views of the leading edge (claudinB:EGFP, bottom left; and immunolabeling against indicated molecule, bottom right). All molecules are properly localized to the apical domains of cells in the leading region of the pLLp, including pLLps in embryos treated with FgfR or MAPKK inhibitors (2 hour treatment, 28-30 hpf). Pink arrowheads in each set of panels indicate the most caudal accumulation of molecule. (D,H,I,P,T) Graphs show quantification of recruitment polarity/cytoskeletal molecules to the apical domains of pLLp cells. Graphs represent percent of pLLp cells that do not display apically localized Par3-TagRFP, γ -tubulin, F-actin, Myosin-II or Cadherin-2. Quantification was performed by manually counting the number of cells in the leading zone that lacked apical localization of indicated molecule. Quantitation was normalized to the total number of cells in the pLLp. There is no significant difference in recruitment of any of these molecules (one-way ANOVA). Scale bar=20 μ m.

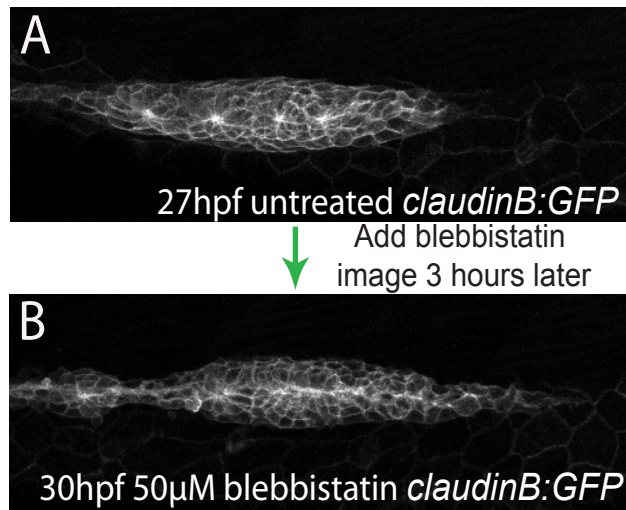


Figure 1.6: Myosin-II is required for rosette formation. Following 3 hours treatment with the Myosin-II inhibitor Blebbistatin, no rosettes have formed in the leading edge of the pLLp (B).

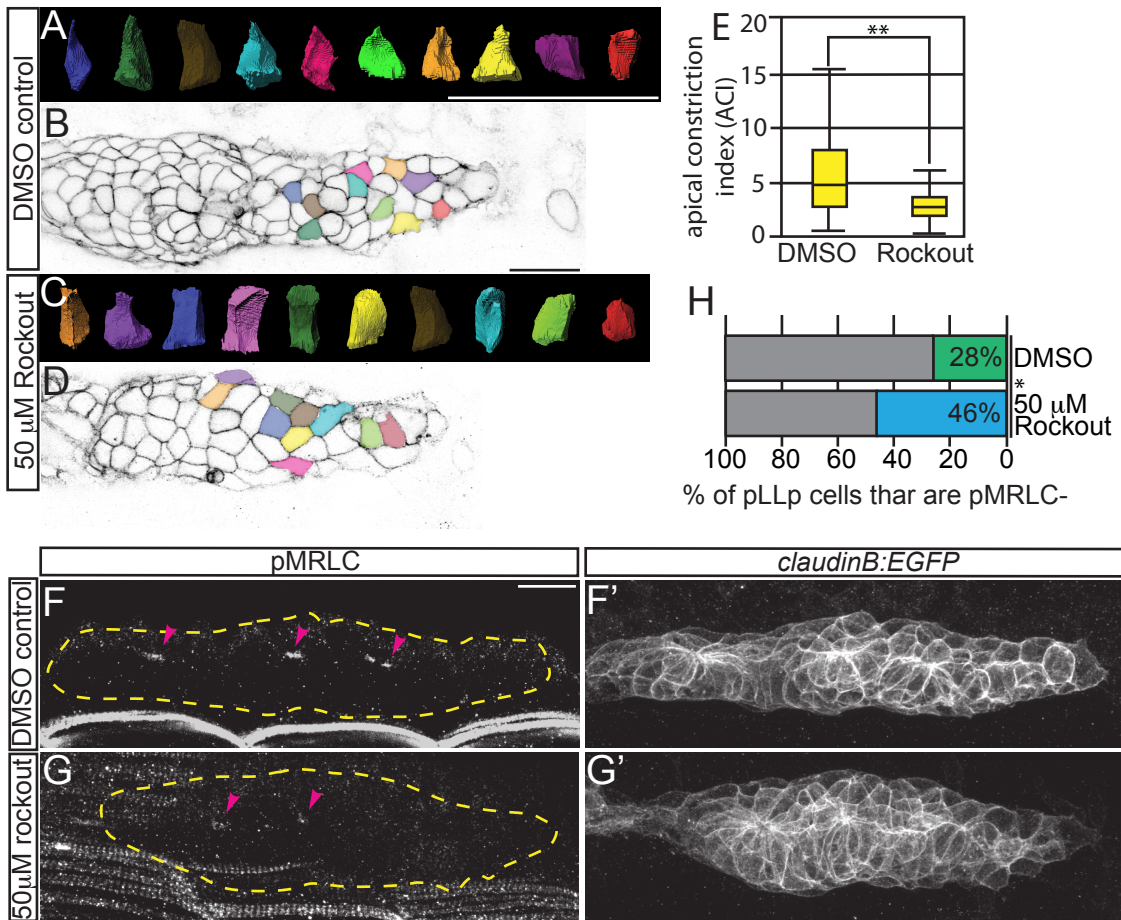


Figure 1.7: Rho-kinase activity is required for rosette formation, apical constriction and MRLC activation. (A-G) *claudinB:EGFP* embryos treated from 28 to 30 hpf with Rho-kinase inhibitor Rockout. ACI were subsequently measured for the leading-most 30 cells (C,D) and compared with DMSO-treated controls (A,B). Colors of surfaces in (A,C) correspond to cell positions in (B,D). (E) ACI measurements from embryos treated with Rockout or DMSO (n=90 cells from 3 embryos/condition; **p<0.0001, Wilcoxon test). (F-G) Immunolabeling showing loss of pMRLC from the leading region following Rockout treatment versus control. (H) Quantification of the leading region, where pMRLC is not detected (*p<0.0001, Student's t-test). Scale bar=20 μm.

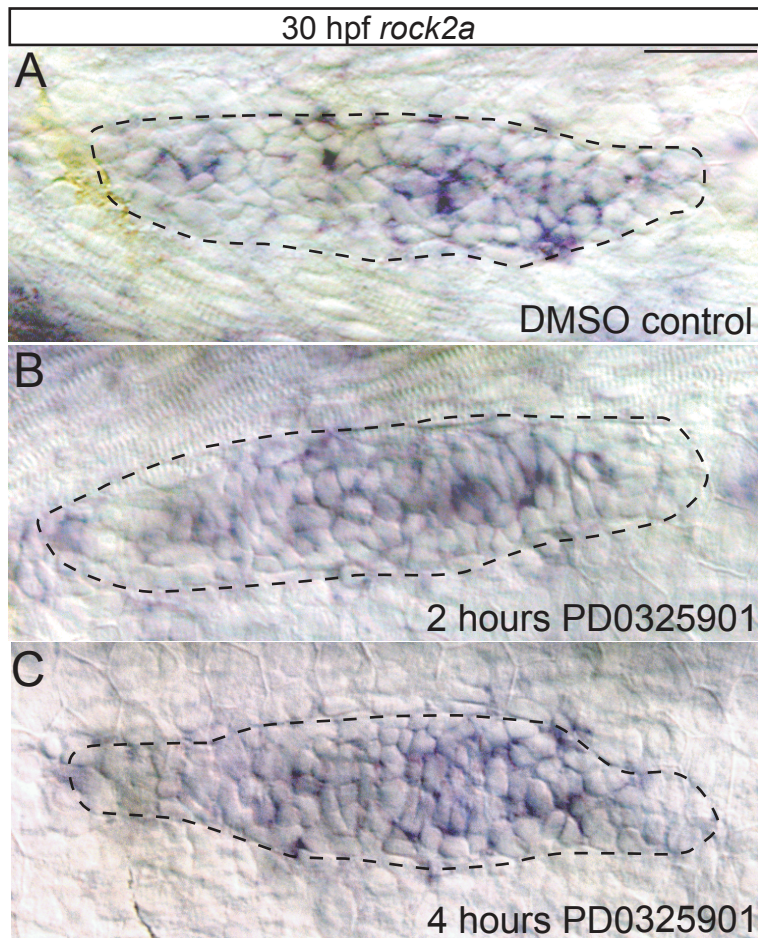


Figure 1.8: MAPK does not regulate levels and distribution of *rock2a* transcript in the pLLp. (A) In situ hybridization against *rock2a* in the pLLp at 30 hpf. The *rock2a* transcript is present throughout the pLLp. (B-C) Inhibition of MAPKK for 2 hours (B) or 4 hours (C) does not change overall levels or distribution of *rock2a*. Scale bar=30 μ m.

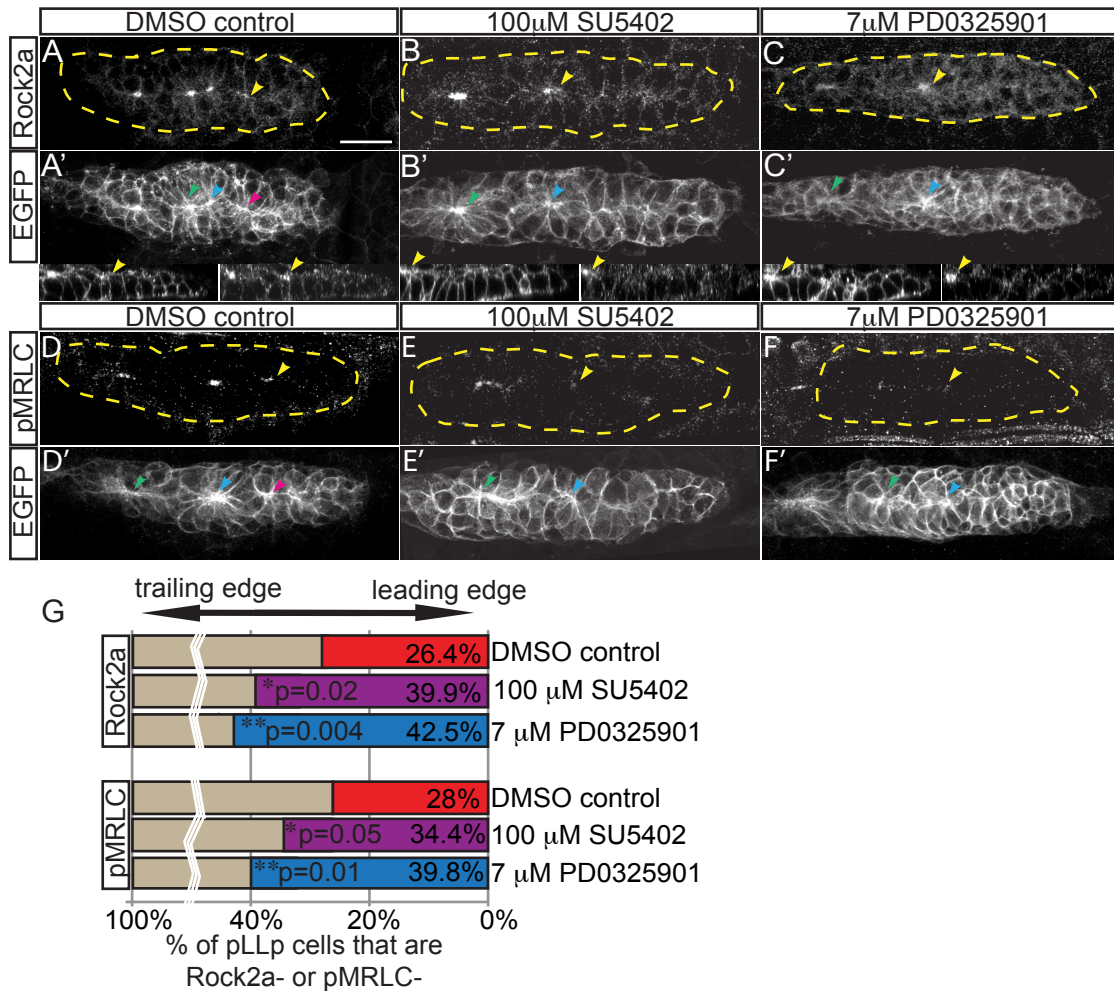
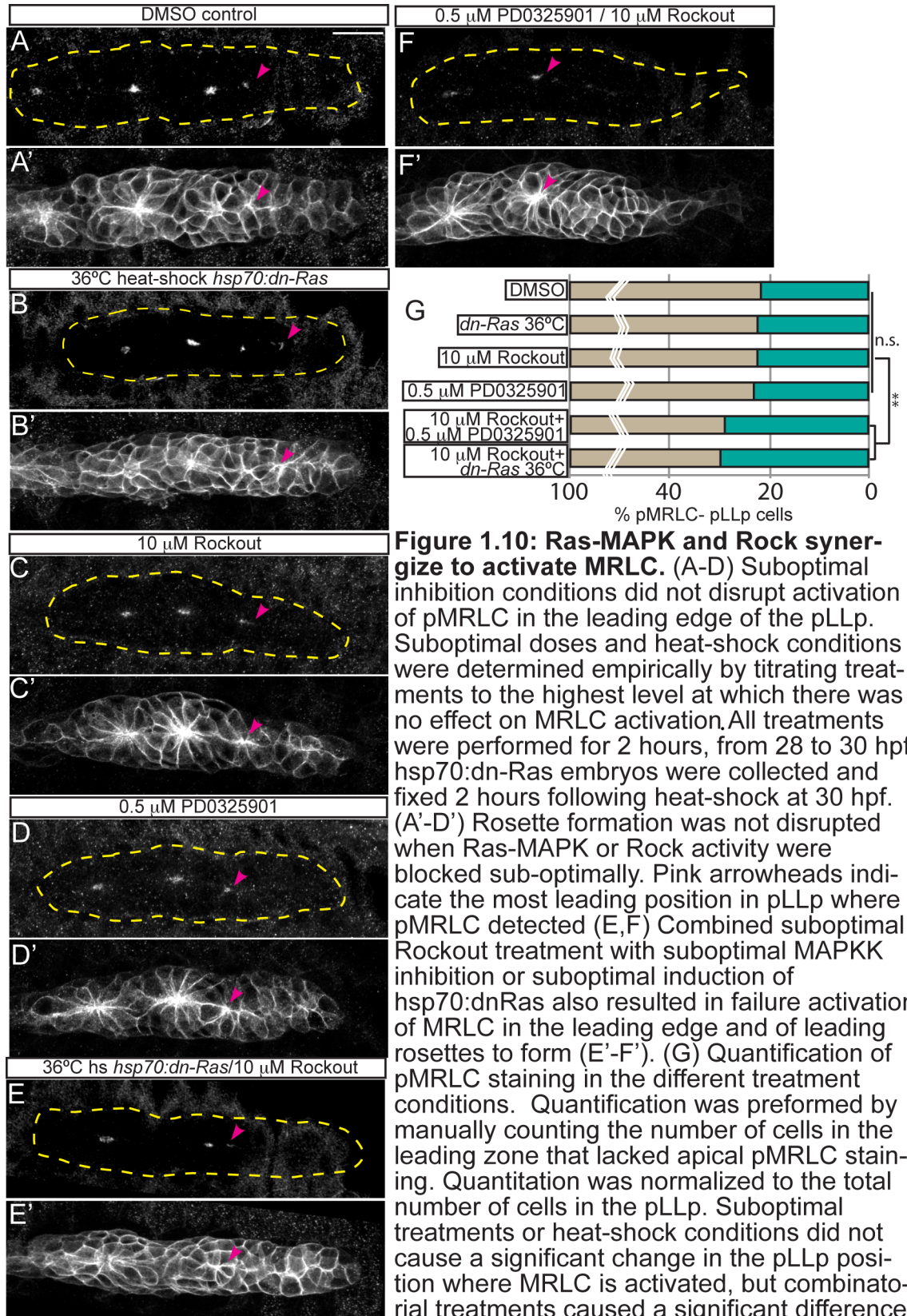


Figure 1.9: Fgf and MAPK signaling are required for localization of Rock2a and MRLC activation. (A-F) FgfR or MAPKK inhibition with SU5402 and PD0325901, respectively, from 28-30 hpf in claudinB:EGFP. Post-treatment, Rock2a (A-C) or pMRLC (D-F) assayed by immunolabeling. Yellow arrowheads indicate caudal-most apical accumulation of Rock2a. Note that Rock2a is not localized to apical ends of cells in the leading region following treatments. pMRLC staining shows failure of leading-region MRLC activation following treatments. (G) Quantification of the leading region. Rock2a (n=6 embryos; $p < 0.03$, ANOVA) and pMRLC (n=6 embryos; $p < 0.003$, ANOVA) are not apically localized. Note there are more leading cells without apically localized Rock2a in Fgf- or MAPKK-inhibited embryos ($39.9 \pm 1.1\%$ and $42.5 \pm 1.4\%$, respectively, versus control ($26.4 \pm 1.5\%$)). For pMRLC staining, DMSO= $28.0 \pm 0.7\%$, SU5402= $34.4 \pm 0.6\%$ and PD0325901= $39.8 \pm 1.0\%$. Scale bar= $20 \mu\text{m}$.



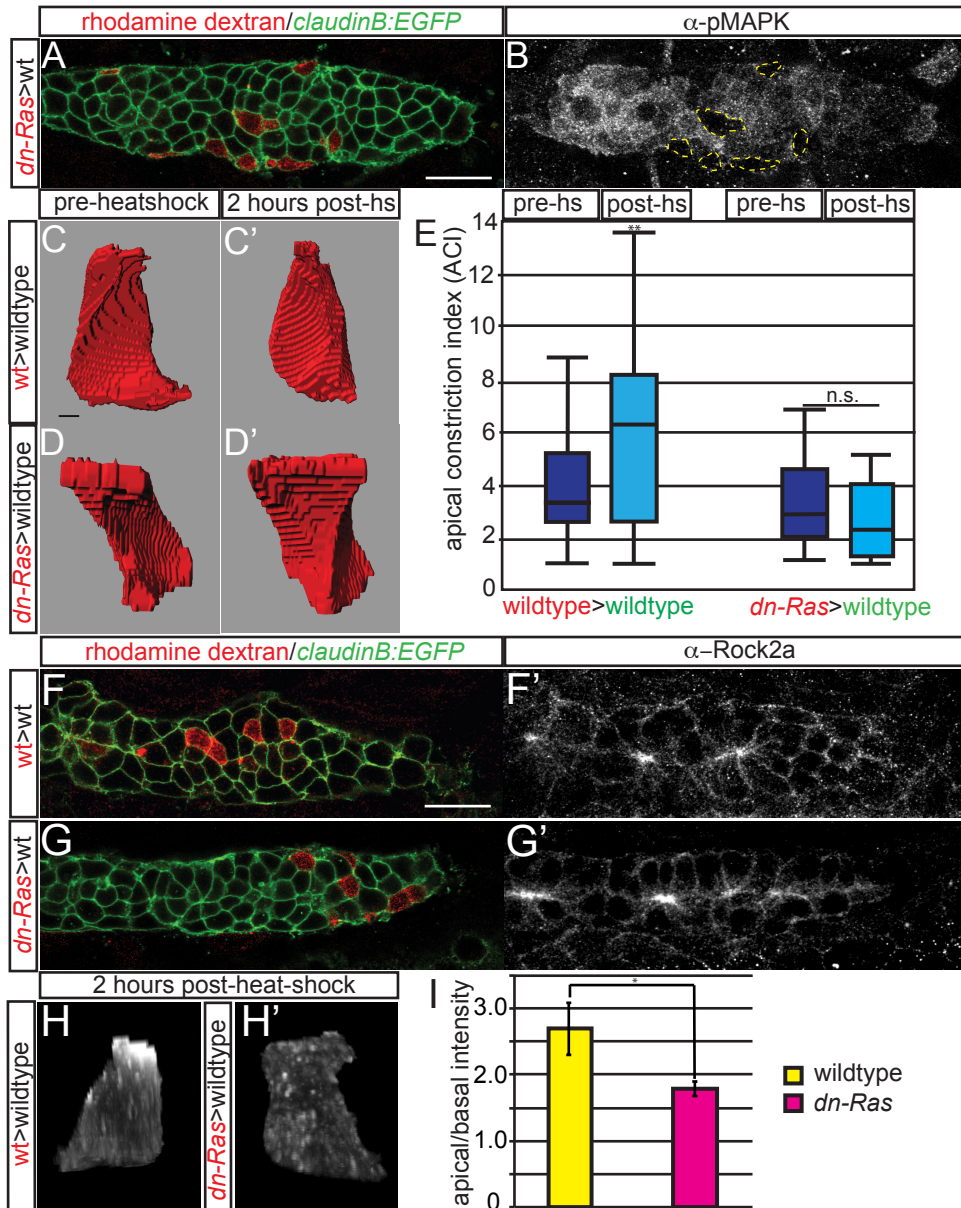


Figure 1.11: Ras-MAPK signaling mediates cell-autonomous apical constriction and Rock2a localization. (A-B) *claudinB:EGFP*-positive mosaic embryos containing *hsp70:dn-Ras* donor cells (red) at 30 hpf. Note lack of pMAPK labeling in *dn-Ras* cells. (C-D) Before heat shock, both *dn-Ras* and wild-type donor cells are columnar; 2-hours post-heat-shock, the wild-type cell is constricted, but *dn-Ras* cell remains columnar. (E) Quantification of ACIs of transplanted wild-type and of *hsp70:dn-Ras* cells before and after heat-shock (Wilcoxon test; ** $p < 0.009$). (F-G) Transplantation of *hsp70:dn-Ras* or wild-type cells causes no obvious difference in global Rock2a distribution. (H) Rock2a distribution in a single transplanted cell shows failure of Rock2a apical localization when Ras is inhibited. (I) Ratio of apical to basal fluorescence intensity in transplanted wild-type cells and *dn-Ras* cells (ANOVA; * $p < 0.03$). Scale bar=20 μm in (B) and 2 μm in (C).

**Chapter 2: Jip-3 dependent Ret localization is
required for proper axon extension.**

Abstract:

During development, neuronal processes extend from the cell body to innervate distal tissues. Axon extension to target tissues is critical for proper development of neuronal circuits. The tyrosine kinase receptor Rearranged in transfection (Ret) has been identified as an important regulator of axon extension. During outgrowth, Ret is localized to the growth cones of extending axons. When Ret is absent or mutated, axons fail to reach innervation targets. However, the molecular machinery that mediates Ret signaling and subcellular localization during axon extension is not understood. In this study, we identified JNK-interacting protein 3 (Jip3) as a mediator of Ret-dependent axon elongation. *jip3^{nl7}* zebrafish mutants show incomplete extension of long axons in the posterior lateral line (pLL) mechanosensory system, reminiscent of Ret-loss-of-function phenotypes. Using immunohistochemistry, genetic manipulations, protein interaction studies and live embryo imaging, we provide evidence that JNK-interacting protein 3 (Jip3) serves as an adapter to link Ret to dynein motor for retrograde transport, a molecular process required for Ret's function in axon extension.

INTRODUCTION:

Neurons have a distinct morphology, characterized by dramatically long processes, termed axons. For proper wiring of neuronal circuits, developing axons, guided by molecular cues, extend over very long distances to properly innervate targets. Often, diffusible growth factors are secreted from surrounding or target tissues to direct proper axon outgrowth. These growth factors, including Nerve Growth Factor (NGF) and Brain-derived Neurotrophic Factor (BDNF), bind to receptor tyrosine kinases (RTKs) positioned in the growth cone (TrkA and TrkB, respectively). These signals can be propagated back to the cell body by endocytosis of the ligand-bound receptor and retrograde transport of the complex. As the distance between cell bodies and the growth cones of extending axons becomes increasingly large over the course of axon outgrowth, developing neurons become increasingly reliant on microtubule based retrograde axonal transport. Other receptor ligand pairs, including Glial-derived Neurotrophic Factor (GDNF)/Ret complex are known to play similar roles in mediating axon extension (Young et al., 2004). Ret is known to be internalized and colocalized with the early endosome marker Rab5a in axon terminals (Richardson et al., 2006). It has been suggested that the Ret/GDNF complex is transported back to the cell body (Richardson et al. 2012). However, whether this is a conserved process and relies on dynein-based retrograde transport and what factors mediate this specific interaction are unknown.

In the zebrafish lateral line, neurons positioned behind the ear in the lateral line ganglion are the afferent mediators of mechanosensation. The long

axons associated with these neurons innervate sensory neuromasts (NMs) that are positioned along the trunk of the zebrafish and relay signals to the Central Nervous System (CNS). These axons extend early in development, between 20-48 hours post fertilization (hpf). At the earliest stages, a subset of these neurons gives rise to pioneer axons whose growth cones are embedded in the posterior lateral line primordium (pLLp), extending along the migratory route of the pLLp (Metcalf 1985; Gilmour et al. 2004). These pioneer axons eventually innervate the most distal terminal cluster NMs. Relative to other pLL neurons, the cells extending pioneer axons differentiate earliest and have a large cell body volume (Pujol-Martí et al. 2012).

The association between pLL pioneers and the migrating pLLp relies on Ret/GDNF signaling. The growth factor GDNF is expressed in the migrating pLLp, while Ret and its co-receptors Gfr α 1a and Gfr α 1b are expressed in the pLL ganglion (Shepherd et al. 2004; Schuster, Dambly-Chaudière, and Ghysen 2010). Combinatorial knockdown of GDNF and Ret using antisense oligonucleotides causes failure of axon extension without affecting pLLp migration, suggesting the Ret/GDNF interaction is required for axon extension (Schuster, Dambly-Chaudière, and Ghysen 2010). In this model, pLL pioneers respond to GDNF by binding to and activating Ret, presumably positioned on the pioneer axon growth cones.

The molecular mechanism by which Ret/GDNF signaling mediates axon outgrowth, and whether this mechanism is dependent on retrograde transport is not currently known. Ret has two dominant alternatively spliced isoforms, Ret9

and Ret51 that differ in their carboxy-termini (Tahira et al. 1990). In *in vitro* models, the two isoforms have been ascribed unique trafficking properties, and both redundant and independent downstream signaling pathways (Douglas S Richardson et al. 2012). In addition, Ret is trafficked differentially in cultured sympathetic versus sensory neurons: activated Ret is rapidly degraded in sympathetic neurons, but is sustained and presents in the cell bodies of Dorsal Root Ganglion neurons, suggesting retrograde transport (Tsui and Pierchala 2010).

Retrograde axonal transport is primarily mediated by a motor cytoplasmic dynein. In contrast to the diversity of anterograde kinesin motors (~40 motors that belong to 14 families), cytoplasmic dynein is the single molecular motor that mediates transport of the majority of retrograde axonal cargo. How this single motor is regulated and transports a diversity of retrograde cargos is not well understood. Recently, multiple molecules have been implicated in mediating and regulating the great diversity of dynein retrograde transport. Several dynein adaptors have been identified, including nuclear distribution protein E (NUDE) and NUDE-like (NUDEL), but a greater diversity of adaptors must exist to facilitate the large diversity of retrograde transport (Kardon and Vale 2009). In addition, Dynein interacting accessory proteins, including the large multi-protein complex Dynactin, are necessary for initiation of retrograde transport (Moughamian and Holzbaaur 2012; Lloyd et al. 2012). Retrograde adaptors are important for linking dynein to specific cargos. One such retrograde adaptor is JNK-interacting protein-3 (Jip-3). Jip-3 has been reported to bind to multiple

components of the dynein complex, including Dynein Light Intermediate Chain and Dynactin complex member p150 (Cavalli et al. 2005).

Our lab has previously shown that Jip3 is an adaptor for retrograde transport of specific cargos during zebrafish neural development, including lysosomes and the active form of the MAP Kinase JNK (Drerup and Nechiporuk 2013). At this time, Jip3 has not been specifically implicated in dynein mediated retrograde transport of other cellular cargos. In addition, Jip3 has also been shown to act as an anterograde adaptor, linking cargoes to kinesin motors for transport from the cell body to axon terminals. For example, Jip3 is known to act as a bridge between the receptor TrkB and kinesin. This interaction is necessary for TrkB transport to the axon periphery in rat hippocampal neurons, which is in turn required for filopodial formation during axon outgrowth (Huang et al. 2011). However, how Jip3 can serve as both an anterograde and retrograde adapter in different contexts is not clear. In this study, we take advantage of the unique characteristics of the long zebrafish posterior lateral line axons to explore regulation of retrograde Ret transport by dynein-adaptor based machinery and the scaffolding protein Jip3.

In this chapter, we define Jip3 as a novel regulator of Ret localization and transport. Using a *jip3* mutant, we show that the *jip3* mutant axon outgrowth phenotype and the Ret mutant phenotype are nearly identical. In the absence of Jip3 activity, activated Ret accumulates abnormally in the growth cones of extending pLL pioneer axons. Using *in vivo* imaging and nerve sever experiments, we demonstrate that the change in activated Ret localization

correlates with a failure in retrograde Ret transport in *jip3* mutants, suggesting that Jip3 is required for retrograde Ret transport. In support of this, we also show that Jip3 interacts with Ret in mammalian cells via the C-terminus of the protein. Finally, we show that the leucine zipper of Jip3, which binds to the dynein subunit p150, is required for Ret localization and axon extension in Jip3 mutants. This suggests a model in which Jip3 must associate with both active Ret and the retrograde motor complex in order to facilitate Ret retrograde transport and promote axon extension.

Materials and Methods:

Zebrafish husbandry and strains

Adult zebrafish were maintained under standard conditions (Westerfield 1995). pLL axon extension was visualized using TgBAC(*neuroD:EGFP*)^{nl1} referred to here as *neuroD:EGFP*. The following mutant lines were used: *ret*^{hu2846} (Knight et al. 2011), *mapk8ip3*^{nl7} (also called *jip3*^{nl7})(Drerup and Nechiporuk 2013).

Plasmids and Injections

Ret9 was amplified and cloned in pCR4 from 5 dpf wildtype zebrafish cDNA using the following primers: F (ATGGGAAGTACGCGGGGA), R (GAATCTAGTAAATGCATGG). *5kbneuroD:Ret9-mTangerine* plasmid was assembled using Multisite Gateway cloning (Obholzer et al. 2008) (Invitrogen and (Invitrogen and Kwan et al. 2007), and microinjected into 1 cell stage embryos at 5 pg/embryo. *Jip3* deletion constructs were derived from pME-Jip3

(Drerup and Nechiporuk 2013) using Quickchange II kit with the following primers: $\Delta p150$ forward (GGGAAAGAAGTGGAAAATGAGGAGCTGGAA TCGGTA), $\Delta p150$ reverse (TTTACCGATTCCAGCTCCTCATTTCCTTCTTTTC), ΔJNK forward (GAGGAAAAGTAAAACAGGTGGAGATGGCAT GGAGGA), $\Delta pJNK$ reverse (CCATGCCATCTCCACCTGTTTTACTTTTCCTC CAGT). mRNA was synthesized using mMessage Machine (Life Technologies) and microinjected at 500 pg/embryo. Mammalian Ret9 was acquired from J. Milbrandt. Mammalian Jip3-GFP was acquired from V. Cavalli. Mammalian *Jip3 $\Delta p150$* was derived from this plasmid using Quickchange II kit with the following primers: $\Delta p150$ forward (CAGGAGAACAGGAGGTCCTGAAAATCCC CATGGCCC), $\Delta p150$ reverse (CGCTGGGCCATGGGGATTTTCAGGACCT CCTGTTCT).

Immunolabeling and in situ hybridization

Immunolabeling was performed following established protocols (Ungos, Karlstrom, and Raible 2003), with the following exception: embryos stained with anti-Ret were fixed in Shandon Glyo-Fixx (Thermo Scientific). Antibodies used: mouse anti-GFP (1:1000; Roche), rabbit anti-Ret (1:100; Santa Cruz), rabbit anti-Retp905 (1:50; Thermo), rabbit anti-Rab5 (1:50, Cell Signaling), rabbit anti-TrkB (1:100; Santa Cruz Biotechnology), rabbit anti-Arf6 (1:100; Sigma). Ret in situ hybridization was performed as described (Andermann, Ungos, and Raible 2002). Isoform specific probes for *ret9* and *ret51* were amplified and cloned into pCR4 TOPO with the following primers: *ret51F*

(GTCATACCCGAACTGGCCAGA), ret 51R (ACTATCGATTGTGTCCACGAT), ret9F (TCCATAGGAAGAGCTGTGATTG), ret9R (GTAAAGACAGGGTTAGTGGCA). In situ-labeled embryos were imaged using Zeiss Axioplan Microscope. Fluorescently-labeled embryos were imaged using an FV1000 confocal (Olympus). Images were processed in ImageJ (Abramoff 2004); brightness and contrast were adjusted in Adobe Photoshop.

Axotomy and Image analysis

Axotomy, immunohistochemistry and fluorescence intensity measurement were performed as described (Drerup and Nechiporuk 2013).

Retrograde labeling of pioneer axons

40 hpf *neuroD:EGFP* embryos were anesthetized and mounted in 1.2% low melt agarose. Tails were severed with rhodamine dextran soaked scissors just rostral to pLLp growth cones. Embryos were freed from agarose, allowed to develop for 3 hours, then re-mounted and imaged using an FV1000 confocal. Embryos were subsequently fixed and stained to detect Ret immunoreactivity.

In Vivo Imaging

In vivo imaging of *Ret9-mTangerine* transport was performed on 30 hpf embryos as previously described (Drerup and Nechiporuk 2013). Kymographs were generated using Metamorph image analysis software (Molecular Devices).

***Mammalian Cell Culture and Co-immunoprecipitation**

HEK293T cells were transfected with 1.25µg of the plasmids described using Lipofectamine2000 (Invitrogen). For co-immunoprecipitation (co-IP), cells were lysed in 200µL of a standard lysis buffer, incubated on ice for an hour, and centrifuged at max speed for 30 min at 4°C. The supernatant was transferred to a new tube and incubated with 0.5µL rabbit anti-GFP antibody (Invitrogen) overnight at 4°C. 15µL of whole cell extract was saved. Pre-washed A/G agarose beads were added for 2 hours at 4°C. Subsequently, beads were pelleted by centrifugation at 1000g for 3 min. Beads were washed 5 times in lysis buffer and then resuspended in laemmle buffer. Protein samples were incubated at 98°C for 10 min and co-IP were centrifuged for 5 min. 10µL of whole cell extracts and 15µL of co-IPs were run on a 12% polyacrylamide gel (Bio Rad) and processed for Western blot analysis.

RESULTS:

The tyrosine kinase receptor Ret is required in the pLL for pioneer axon outgrowth

Combinatorial knockdown of Ret and GDNF suggests that pLL axon outgrowth relies on Ret/GDNF signaling (Schuster, Dambly-Chaudière, and Ghysen 2010). To confirm that Ret plays an important role in axon outgrowth, we immunostained axons of 3dpf *ret*^{hu2846} mutant embryos (early stop codon) with a neurofilament marker, α-3A10. We observed a failure of complete axon extension

* Catherine Drerup, Ph.D, preformed the work described in this section.

in 100% of *ret*^{hu2846} mutants when compared with wildtype (Fig. 2.1A,B). As these experiments revealed a critical role for Ret in axon outgrowth, we examined the subcellular localization of Ret in pLL neurons. We found that Ret is expressed in a subset of pLL neuronal cell bodies during axon extension, 30 hpf (Fig. 2.1C).

We asked whether the Ret-expressing pLL neurons represent the cell bodies of pioneer axons. By clipping tails of 40 hpf *neuroD:EGFP* transgenic embryos with rhodamine dextran soaked scissors, we specifically labeled the cell bodies of the longest, pioneer pLL axons. We found that the majority (8 of 10 cells analyzed from n=5 embryos) of rhodamine dextran labeled pioneer axons also labeled with the α -Ret antibody (Fig. 2.2A-C), supporting a role for Ret signaling in pioneer axon outgrowth.

Jip3 is required for axon outgrowth and Ret localization

Using chemical mutagenesis, our lab previously identified a zebrafish line which had a null-mutation in JNK-interacting protein 3 (*jip3*^{nl7}; Drerup and Nechiporuk 2013). These mutants display partially penetrant truncation of the lateral line axons (Drerup and Nechiporuk 2013), at an axial level similar to that observed in *ret* mutants, though the molecular underpinnings of this phenotype is not understood. We asked whether Jip3 might play a role in regulating Ret, so we immunostained *jip3* mutants at 30 hpf (during the midpoint of pLL axon extension) with the α -Ret antibody. *Jip3* mutant embryos show a distribution of Ret in the pLL cell bodies similar to wildtype siblings (Fig. 2.1E,E'). In contrast,

jip3^{nl7} mutants displayed dramatic accumulations of Ret in growth cones (Fig. 2.1F,F'), potentially suggesting failed retrograde transport of Ret. To determine whether this pool represented the active (phosphorylated) form of Ret, we stained *jip3^{nl7}* mutant embryos with α -pRet905. In comparison to wildtype, *jip3^{nl7}* mutants displayed accumulations of pRet905 (Fig. 2.1G-H), indicating that the Ret accumulations in Jip3 growth cones represent an activated pool of Ret.

We wondered whether the accumulation of Ret in growth cones represented a global failure in retrograde axonal transport in *jip3^{nl7}* mutants at 30 hpf. To test this, we examined localization of other molecules, including the receptor tyrosine kinase TrkB and the Jip3 effector Arf6 (Suzuki et al. 2010). We observed similar distribution of Arf6 in growth cones of wildtype and *jip3^{nl7}* embryos at 30 hpf (Fig. 2.3A,B). We observed a slight, non-significant reduction in TrkB in growth cones of wildtype and *jip3* mutant embryos at 30 hpf (Fig. 2.3C,D). This data suggests that the change in Ret distribution is due to a specific role for Jip3 in Ret localization, and not a global disruption in axonal transport.

Jip3 is required for Ret transport

Because Jip3 mutants displayed accumulations of Ret and pRet in growth cones, we next determined if Jip3 was required for retrograde transport of Ret. We first tested whether Ret and/or pRet accumulates at the distal site of nerve sever, an indirect measure of retrograde axonal transport (Fig. 2.4; Drerup and Nechiporuk 2013). While there was no accumulation of pRet at the site of the

proximal cut (Fig. 2.4A-C), pRet accumulated at the distal cut site (Fig. 2.4D-F) in wildtype embryos. In contrast, *jip3^{nl7}* mutants showed a failure of pRet accumulation, strongly implying that Jip3 is required for retrograde pRet transport (Fig. 2.4D-F). Note that there was no change in total Ret accumulation at the site of either the proximal or distal cut. This result also suggests that Jip3 may preferentially transport the activated form of Ret.

Several distinct isoforms of Ret are expressed in the nervous system (Tahira et al. 1990). In order to determine which isoform of Ret is relevant during pLL axon extension, we performed *in situ hybridization* against the most prevalent isoforms of *ret*, *ret9* and *ret51* (Fig. 2.5D-F). These experiments showed expression of *ret9*, but not *ret51* in the pLLg at 30 hpf. We therefore performed all subsequent experiments using the *ret9* isoform.

Next we assayed Ret transport in real time to determine if active Ret retrograde transport is impaired with loss of Jip3. Previously, our lab developed a technique to analyze axon transport *in vivo* in pLL axons (Drerup and Nechiporuk 2013). To directly look at Ret transport, we transiently expressed a *ret9-mTangerine* fusion, driven by the *5kbneuroD* promoter (Obholzer et al. 2008). Mosaic expression of this construct during axon extension revealed accumulation of Ret9-mTangerine in growth cones of *jip3^{nl7}* mutants (Fig. 2.6B,B'), but not wildtype embryos (Fig. 2.6A,A'), similar to Ret accumulation phenotype observed by immunostaining (Fig. 2.1). Detailed analysis of Ret9 axonal movements showed slight or no defects in distance and velocity measurements in the distal axons of *jip3^{nl7}* embryos in both the anterograde and retrograde directions (Fig.

2.6H,I). However, the frequency of Ret retrograde transport was reduced, suggesting that Jip3 is critical for retrograde Ret transport (Fig. 2.6G). Interestingly, there was also a reduction in anterograde transport frequency (Fig. 2.6G), pointing to a potential role for Jip3 in the anterograde transport of this receptor. This is not surprising considering Jip3's known role in TrkB anterograde transport; however, this impairment in anterograde Ret movement is not severe enough to deplete this receptor from *jip3^{nl7}* axon terminals (Fig. 2.1F'), suggesting that the observed axonal phenotypes are not a result of this slight impairment in anterograde movement. Together, the results of the live imaging and nerve sever analyses suggest that Jip3 is a critical mediator of retrograde movement of active Ret during axon outgrowth.

Rab5 does not accumulate in growth cones of *jip3^{nl7}* mutants

Rab5 is a small GTPase, commonly found on early endosomes, thought to be important in endocytosis and sorting for axonal transport. Previously, Jip3 was implicated in regulation of Rab5 at synaptic terminals (Brown et al. 2009). To test whether deregulation of Rab5 played a role in Ret accumulation in pLL growth cones, we examined Rab5 localization in wildtype and *jip3^{nl7}* mutant embryos. Immunostaining against Rab5 showed no obvious change in distribution between wildtype and *jip3^{nl7}* mutant embryos (Fig. 2.7A,B). We confirmed this with overexpression of *5kbneurod:mTangerine-Rab5c* (Fig. 2.7C,D). This data suggests that accumulation of Ret is not caused by global deregulation of Rab5 distribution.

Jip3 interacts with Ret independently of dynein*

Given the changes we observed in Ret localization and transport in *jip3^{nl7}* mutants, we hypothesized that Jip3 might be acting as a retrograde adaptor, linking Ret to dynein for retrograde transport. To test whether Jip3 and Ret9 physically interact, we overexpressed Jip3-GFP and Ret9 in HEK293 cells. Co-immunoprecipitation of Ret9 by Jip3 revealed a strong interaction between these proteins (Fig. 2.8A).

Next we asked whether the Jip3-Ret interaction is independent from a previously reported Jip3 binding to p150 subunit of dynactin (Cavalli et al. 2005). To test this, we performed a co-IP experiment between Ret and Jip3 that lacked p150 binding domain. Overexpression of Jip-3 lacking the p150 binding domain caused no reduction in the Jip-3-Ret interaction (Fig. 2.8A), indicating that the p150 binding domain is not required for Jip-3's interaction with Ret.

The Jip-3 p150-binding domain is required for axon extension and Ret localization

If Jip3-mediated retrograde transport of Ret is required for axon extension, we expect that the Jip3-dynein interaction would also be required for Ret-dependent axon extension. To test this, we injected mRNAs encoding full length Jip3 (control), Jip3 lacking the p150 binding domain (*jip3 Δ p150*) or Jip3 lacking the JNK interacting domain (*jip3 Δ JNK*) into 1-cell stage embryos derived from a

* Catherine Drerup, Ph.D, preformed the work described in this section.

jip3^{nl7}/+ heterozygous crosses. Full-length Jip-3 and *jip3ΔJNK* were able to completely rescue both Ret localization and axon truncation at 3 dpf (Fig. 2.8B-E). In contrast, *jip-3Δp150* failed to rescue either localization of Ret or axon truncation (Fig. 2.8B). Altogether, these data indicate that the Jip3-p150 interaction is required for Jip3 dependent axon extension as well as proper Ret localization in axon growth cones, arguing for hindered Ret retrograde transport as causal in the axon truncation phenotype observed in *jip3* mutants. However, Jip3 interaction with JNK, which has been previously implicated in axon extension (Sun et al. 2013), is not necessary for pLL axon extension.

Discussion

Based on the data presented here, we propose a model in which Jip-3 serves as an adaptor protein, linking Ret to dynein for retrograde transport (Fig. 2.9). This model is based on biochemical and *in vivo* data showing that Jip3 and Ret are physically associated and that Ret transport is dependent on Jip3. For formation of this complex, a yet unidentified Ret-binding domain in Jip-3 exists. In the future, we will identify the minimal Ret-binding domain in the Jip-3 amino acid sequence, using both co-immunoprecipitation from mammalian cells and rescue analyses using Jip3 deletion constructs in zebrafish embryos. In addition, we will perform co-transport experiments, to visualize co-transport of Ret and Jip-3 double-positive vesicles. We suggest that assembly of this Ret-Jip-3-Dynein complex is required for retrograde transport of Ret, a cellular activity necessary for Ret-dependent axon extension.

Ret/GDNF signaling during pLL axon extension

Because of the previously described role for Ret/GDNF signaling in lateral line axon extension, we were initially surprised by the relatively late truncation of the *ret*^{hu2846} mutant pLL axons. This phenotype suggests that Ret is required only for the final stages of axon extension. Interestingly, the severity of the axon truncation phenotype is similar between the *ret*^{hu2846} and *jip3*^{nl7} mutants; This similarity suggests that Ret-dependent axon extension absolutely requires Jip3 activity. Perhaps in wildtype conditions, Jip3-dependent retrograde transport of Ret results in delivery to the cell body when axon extension is nearly complete, and this signal promotes the final stages of complete axon outgrowth. In contrast, the lack of retrograde delivery of Ret to the cell body in *jip3*^{nl7} mutants results in incomplete axon extension. It is also interesting to note that the truncation phenotype in *jip3*^{nl7} mutants is not fully penetrant, suggesting that Jip3-dependent Ret transport might not be absolutely required. Alternatively, perhaps Jip3 can be compensated for by a second dynein adaptor.

Additionally, a downstream molecular response is likely directly involved in Ret-dependent axon outgrowth in the pLLp. Following arrival in the cell body, Jip3-transported Ret likely activates intracellular signaling or transcriptional activity. Previously, MAPK/ERK and PI3K signaling have been identified as downstream mediators of Ret activation (D S Richardson, Lai, and Mulligan 2006). Our preliminary experiments failed to detect differences in levels of pMAPK in the cell bodies of pLL neurons between wildtype and *jip3*^{nl7} mutants

(data not shown). However, additional experiments are required to confirm this result. While identification of the molecules that act downstream of Ret during pLL axon extension is beyond the scope of this study, future studies in the lab will aim to ascertain candidates that may be important in activation of membrane trafficking, actin dynamics or microtubule assembly. In pursuing these experiments, we must note that the different isoforms of Ret, Ret9 and Ret51, have been shown to have differential signaling capacities based on the amino acid sequences and phosphorylation sites in their divergent C-termini.

A role for Jip3 in Ret anterograde transport?

Unexpectedly, *jip3^{nl7}* mutants displayed a reduction in both retrograde and anterograde Ret transport frequency. This result raises several additional questions. First, does Jip3 have a role in Ret anterograde transport? While our nerve sever experiments (performed at 5 dpf) showed no difference in proximal accumulation of Ret or pRet, *in vivo* transport data at 30 hpf demonstrated a clear reduction in anterograde Ret9-mTangerine transport frequency in *jip3^{nl7}* mutants at 30 hpf. These conflicting results suggest that there may be a developmental difference in Ret transport. Whether the disruption in anterograde Ret transport at 30 hpf is due to a direct, loss-of-Jip-3 effect, or is a secondary effect of impaired axon outgrowth is currently unclear. Additionally, it is possible that overexpression of Ret, a factor critical for axon extension, might trigger a feedback loop that reduces the number of Ret-containing vesicles to the extending growth cones. Comparing Ret transport to transport of another, non-Jip-3 dependent cargo would help resolve this question. Additionally, our

proposed Jip-3-Ret co-transport experiments will help identify whether Ret moving in the anterograde direction is associated with Jip-3. Secondly, our observed attenuation in anterograde transport may not be sufficient to stall axon extension, because a sizable portion of Ret is still delivered to axon growth cones. How is a reduced anterograde transport frequency sufficient for delivery of Ret to growth cones, but a similar reduction in retrograde transport frequency completely abolishes Ret-dependent axon outgrowth? Our nerve sever experiments suggest that Jip-3 might be preferentially mediating transport of activated (phosphorylated) Ret in the retrograde direction. Thus, anterogradely and retrogradely Ret populations may represent differently inactive vs. active Ret pools, respectively, explaining the differential consequences of the reduction in anterograde versus retrograde transport of Ret.

Is Jip3-Ret interaction activity dependent?

As previously discussed, our nerve sever experiments suggest that Jip-3 might be preferentially transporting of activated Ret in the retrograde direction. We have designed future experiments to test whether Ret activation is required for Ret-dependent axon extension and Jip3 interaction. By overexpression of mRNAs encoding wildtype or phospho-mutant *ret* in *ret*^{hu2846} mutants, we will ascertain whether non-phosphorylatable forms of Ret are able to rescue the Ret mutant axon truncation phenotype. Because there are multiple phosphorylation residues in the Ret9 c-terminus, we have individually mutated these residues. Identification of a phospho-residue in the Ret C-terminus that is required for Ret dependent axon extension would suggest that Ret activation/phosphorylation is

necessary for axon extension. Additionally, the result of this experiment might help elucidate potential downstream targets, based on previous literature. Finally, if we identify an important phospho-residue(s), we can also test whether phosphorylation at this site is required for Jip-3-Ret interaction, using both biochemical and *in vivo* approaches.

Ret signaling in other species

Ret signaling has been most carefully studied in enteric nervous system, as Ret mutations are correlated with the highest proportion of cases in Hirschsprung's Disease (McKeown et al. 2013). Hirschsprung's is a developmental gastrointestinal disorder, characterized by an absence of enteric neurons from the distal bowel, with Ret apparently acting as a pro-proliferative signal for enteric neuron progenitors (Laranjeira and Pachnis 2009). Interestingly, this role seems distinct from the axon extension requirement for Ret described here and in other central and peripheral nervous system examples (Jiao et al. 2011; Schuster, Dambly-Chaudière, and Ghysen 2010). Interestingly, in zebrafish, Jip3 is expressed in the central and peripheral nervous system, but not in enteric neurons (Dreup and Nechiporuk, unpublished data). This suggests that the Ret-Jip3 interaction described here does not occur in the developing enteric nervous system. Despite this, it will be interesting to determine whether the Ret-Jip3 interaction is conserved in other neuronal populations in which these two proteins are co-expressed. Intriguingly, the relevance of Jip3 in axon outgrowth has recently been appreciated in hippocampal and cortical neurons (Sun et al. 2013), suggesting that Jip3 could play a similar role in these populations. Additionally,

Jip3 null animals lack a telencephalic commissure, suggesting Jip3-dependent axon elongation may occur *in vivo* (Kelkar et al. 2003).

Conclusion

In conclusion, this work has elucidated a novel interaction between the scaffolding protein Jip3 and the RTK Ret. We have shown that this interaction is biologically significant during axon extension, in the context of the zebrafish lateral line and is conserved in mammalian cell culture models. An understanding of how proteins are trafficked on the subcellular level and the physiological relevance of this process is critical for a complete understanding of the morphological changes that occur during development. Additionally, our work shows that appropriate transport and localization of Ret receptor is absolutely required for Ret activity, and this may represent a more general feature of receptor tyrosine kinases.

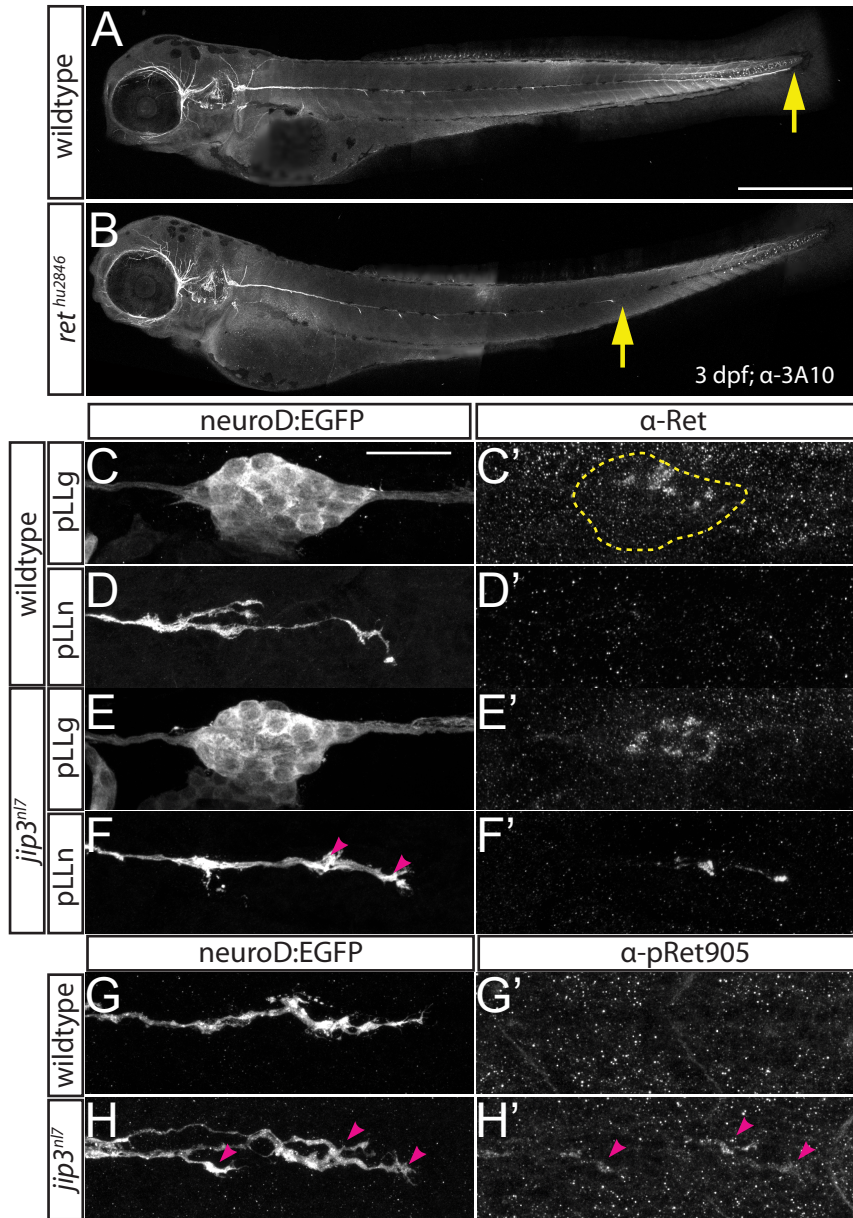


Figure 2.1: Ret is required for complete axon extension and is improperly localized in *jip3^{nl7}* mutants. (A,B) α -3A10 neurofilament immunostaining in 3 dpf wildtype and *ret^{hu2846}* mutants. Yellow arrows mark end of pLL. Scale bar = 500 μ m. (C-F) *neuroD:EGFP* fill and (C'-F') α -Ret immunostaining in the pLLg (C,E) and pLLn growth cones (D,F) of 30 hpf wildtype and *jip3^{nl7}* mutants. Pink arrowheads indicate accumulations of Ret. (G-H) *neuroD:EGFP* fill and (G'-H') α -pRet905 immunostaining of 30 hpf wildtype and *jip3^{nl7}* mutant pLLn growth cones. Pink arrowheads indicate accumulations of pRet905. Scale bar = 30 μ m in (C-H).

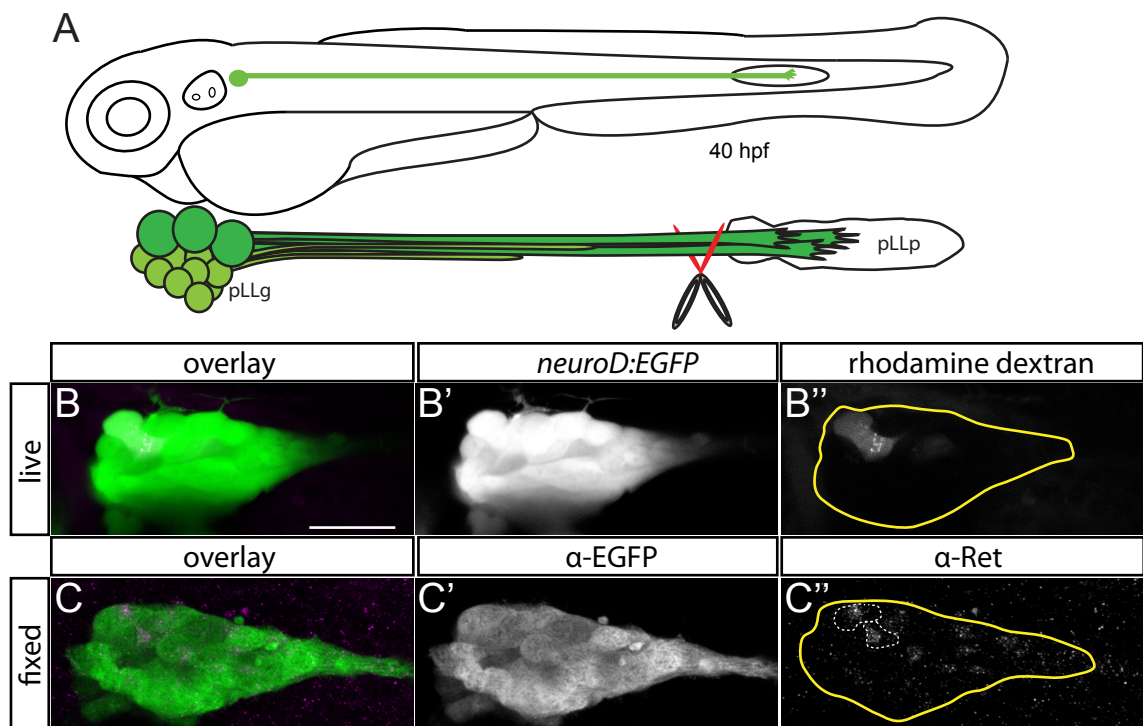


Figure 2.2: Ret is expressed in pioneer axons during axon extension. (A) Experimental set up for retrograde labelling of pioneer axons. Tails of 40 hpf embryos expressing *neuroD:EGFP* were severed using rhodamine dextran soaked scissors. (B) Rhodamine dextran labels anterior dorsal pLLg cells, imaged 3 hours following retrograde labeling of pioneer axons. (C) α -Ret immunostaining labels the same cells. Scale bar = 30 μ m.

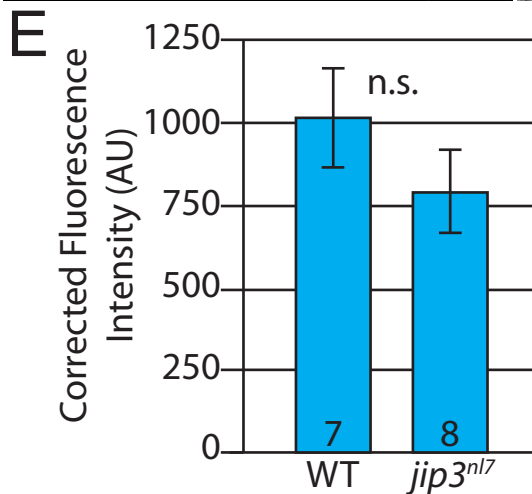
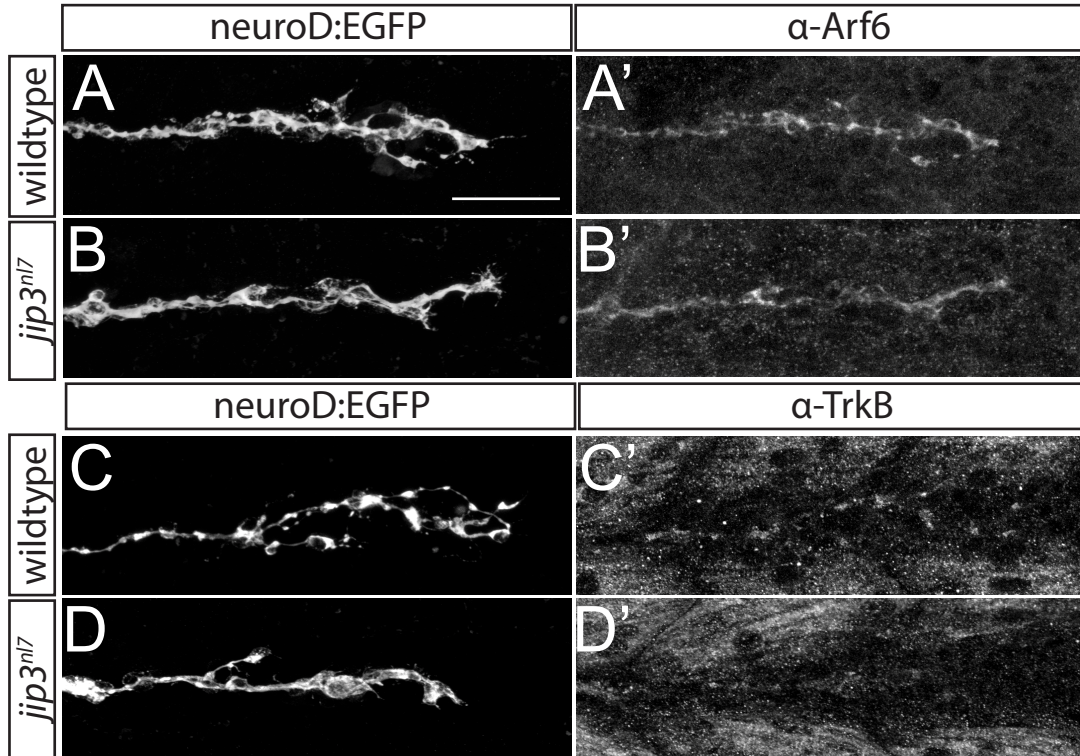


Figure 2.3: Other cargoes do not accumulate in growth cones at 30 hpf in *jip3^{nl7}* mutants. (A,B) *neuroD:EGFP* cell fill and (A',B') α -Arf6 immunostaining in 30 hpf wildtype and *jip3^{nl7}* mutants. (C,C',D,D') α -TrkB immunostaining in 30 hpf wildtype and *jip3^{nl7}* mutants. (E) Quantification of TrkB staining in 30 hpf wildtype and *jip3^{nl7}* mutant growth cones, with background subtraction. Scale bar = 30 μ m.

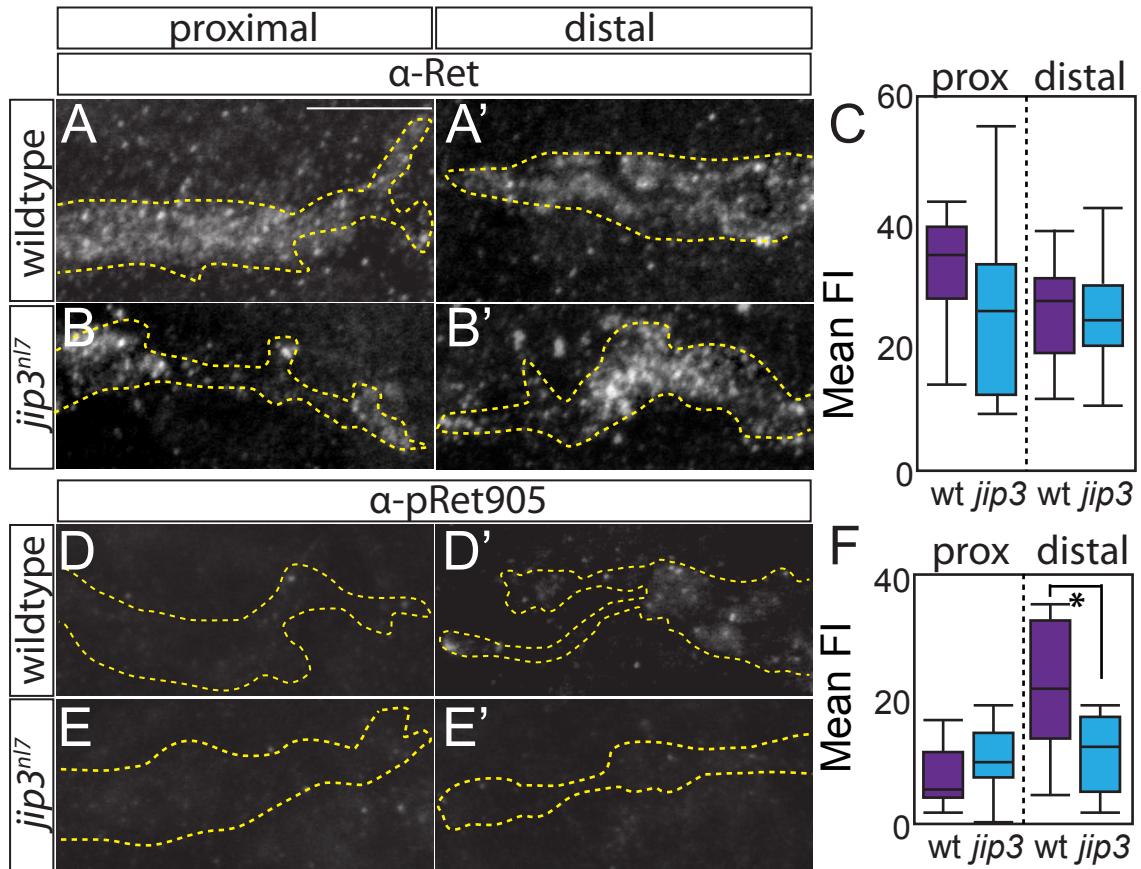


Figure 2.4: pRet accumulates at the site of distal nerve sever in wild-type larvae, but not in *jip3^{nl7}* mutants. (A,B) α -Ret immunostaining of the proximal (A,B) and distal (A',B') cut site of 5 dpf wildtype and *jip3^{nl7}* mutant larvae, fixed 3 hours post-sever. Nerves were severed between NM2 and NM3. (C) Quantification of fluorescence intensity (normalized to background) from α -Ret immunostaining (no significance, two-way ANOVA. wildtype n=12; *jip3^{nl7}* n=14). (D,E) α -pRet905 immunostaining of the proximal (D,E) and distal (D',E') cut site of 5 dpf wildtype and *jip3^{nl7}* mutant larvae, fixed 3 hours post-sever. (F) Mean fluorescence intensity (normalized to background) of α -p905Ret immunostaining of the proximal and distal nerve sever. * $p < 0.005$ (ANOVA) (wildtype n=12; *jip3^{nl7}* n=12). Scale bar=10 μ m.

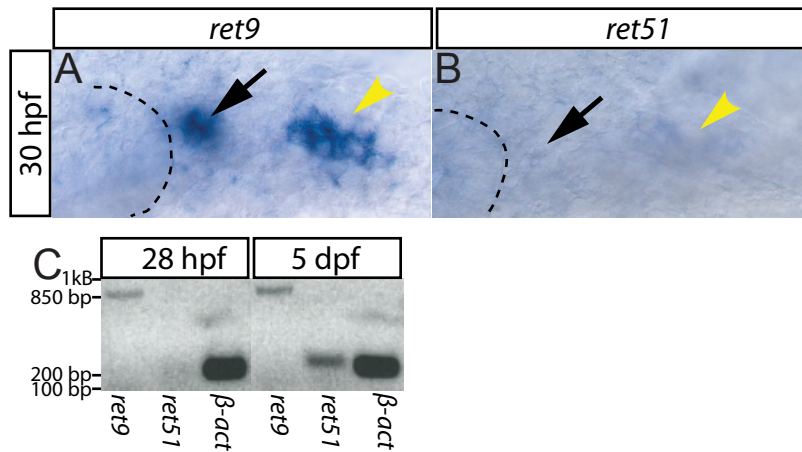


Figure 2.5: Ret9 is expressed in the pLLg during axon extension. (A) *ret9* but not *ret51* (B) is expressed during axon extension (30hpf) in the pLLg. Arrowhead=pLLg; Arrow=middle LLg; dashed line=otic vesicle. (C) RT-PCR at from cDNA collected from wildtype embryos at 28 hpf and 5 dpf.

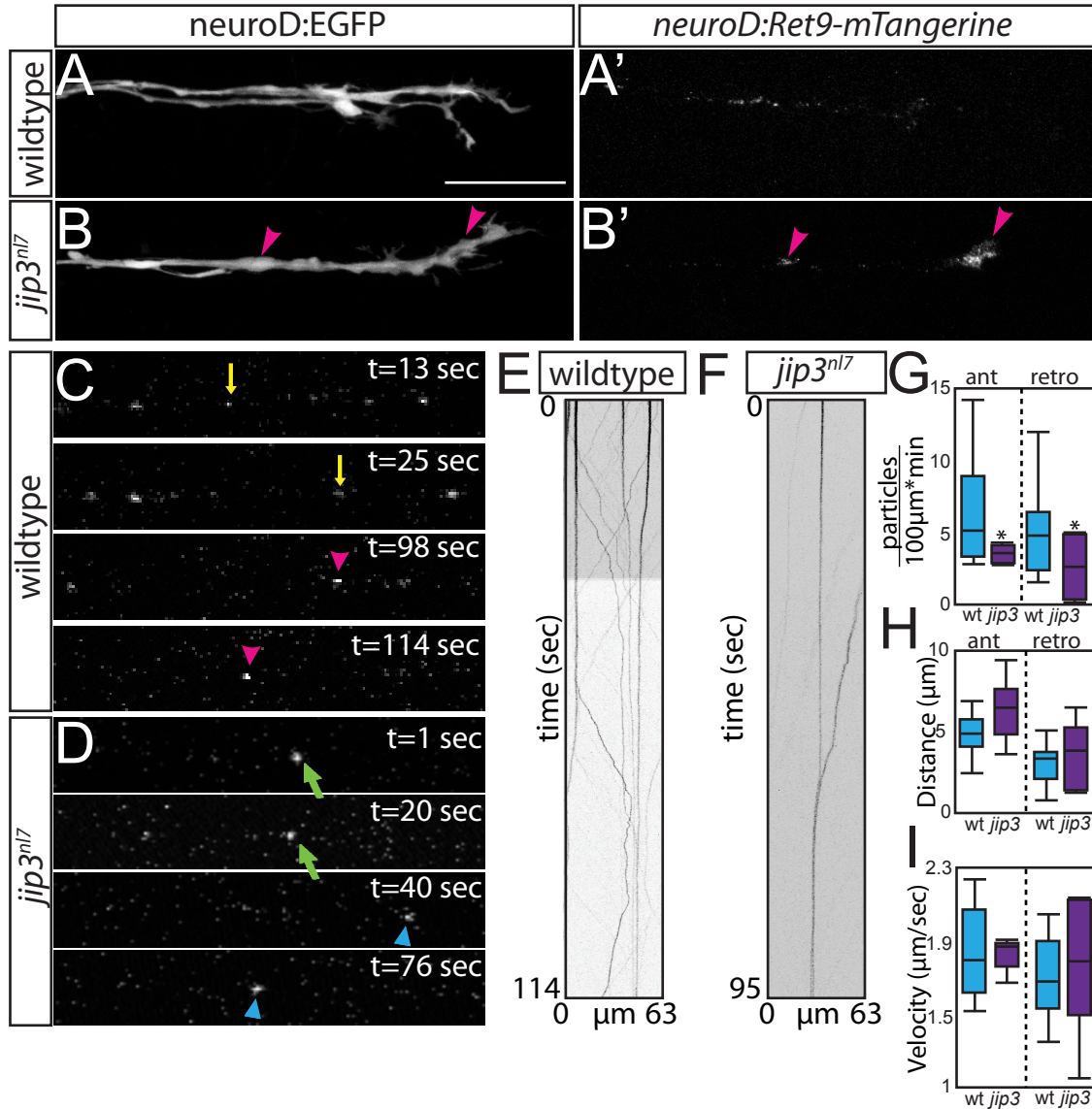


Figure 2.6: Ret transport during axon extension in wildtypes and *jip3^{nl7}* mutants. (A,B) Expression of neuroD:Ret9-mTangerine in 30 hpf wildtype and *jip3^{nl7}* mutant embryos. Pink arrowheads indicate Ret9-mTangerine accumulation in growth cones of *jip3^{nl7}* mutants. (C) Transport of Ret9-mTangerine. Yellow arrows indicate anterograde transport. Pink arrowheads indicate retrograde transport. (D) Transport of Ret9-mTangerine in *jip3^{nl7}* mutants. Green arrows label stationary particle. Blue arrowheads indicate retrograde transport. (E) Kymographs derived from wildtype and (F) *jip3^{nl7}* mutant Ret9-mTangerine transport data. (G) Ret9-mTangerine transport frequency in anterograde and retrograde directions (* $p < 0.05$, two-way ANOVA). No significant differences were observed for anterograde or retrograde distance measurements (H) and or velocity measurements (I). Scale bar = 30 μm.

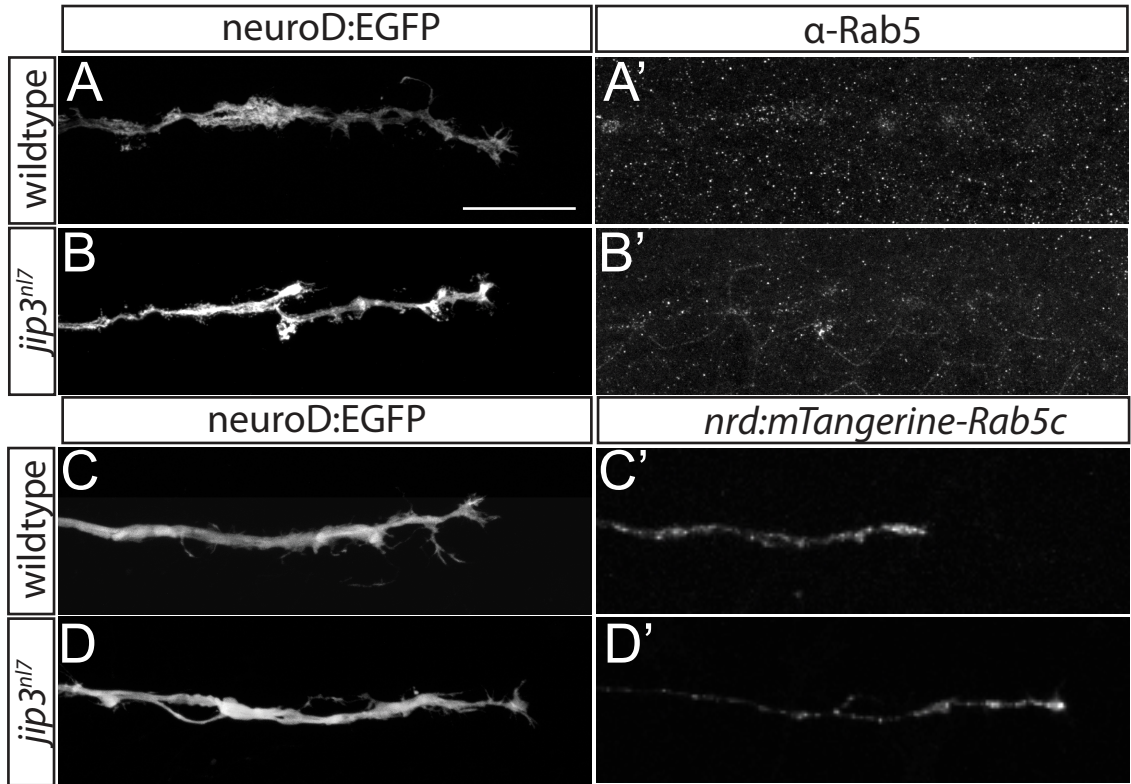
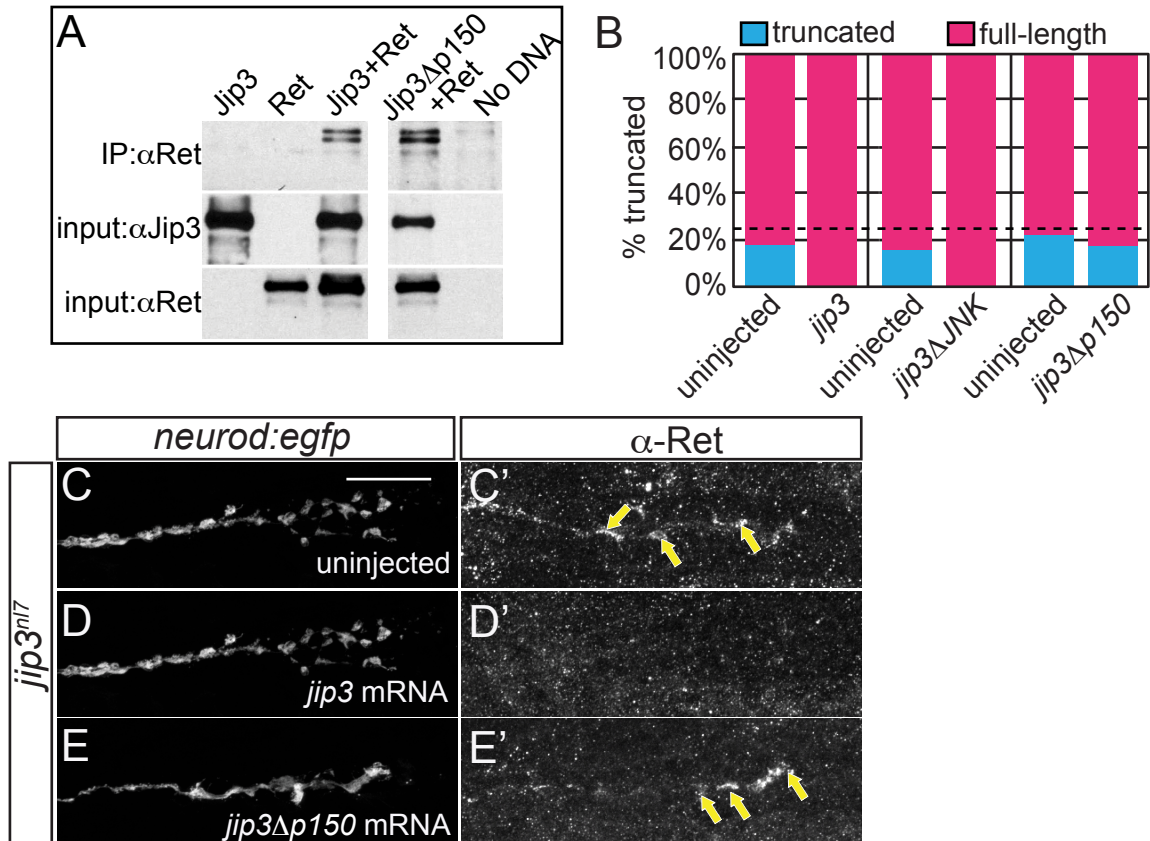


Figure 2.7: Rab5 does not accumulate in growth cones at 30 hpf (A,B) *neuroD:EGFP* cell fill and (A',B') α -Rab5 immunostaining in 30 hpf wildtype and *jip3^{nl7}* mutants. (C,C',D,D') Expression of *nrd:mTangerine-Rab5c* in 30 hpf wildtype and *jip3^{nl7}* mutants. Scale bar = 30 μ m.



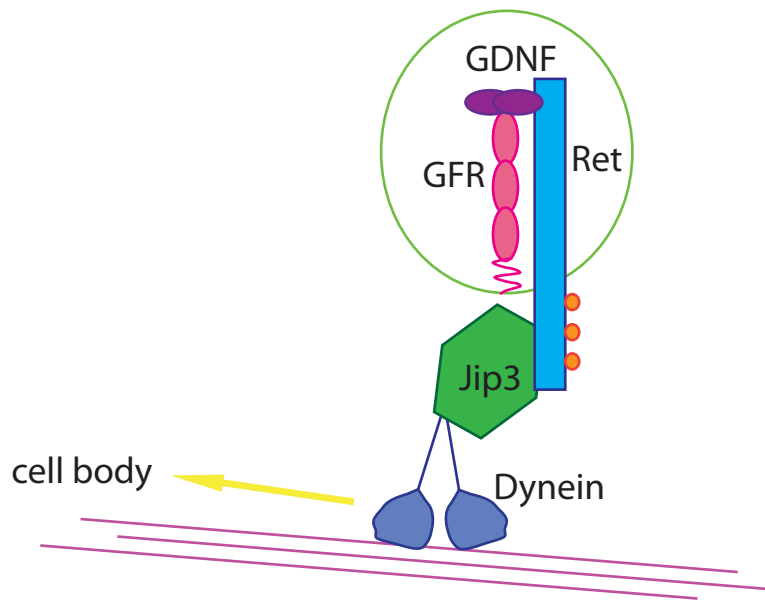


Figure 9: Model for Jip3's role as a retrograde adaptor for Ret. Jip-3 binds to both Ret and Dynein. Binding to both molecules is necessary for assembly of the complex and proper localization of Ret. Note that phosphorylation of Ret (represented by orange circles) may or may not be requisite for Jip-3 dependent retrograde transport.

Chapter 3: Conclusions and Future Directions

Changes in cell morphology are required to form functional adult organ systems, including sensory systems. In this thesis, I have used the developing sensory system of zebrafish to study two distinct cell shape changes: apical constriction and axon extension. My studies revealed molecular signals that coordinate specific aspects of these cell shape changes. Chapter 1 showed how extracellular signals could be transmitted intracellularly to induce apical constriction, a cell shape change necessary for formation of multicellular rosettes. In chapter 2, I showed that the interaction between the RTK Ret and the scaffolding molecule Jip3 was required for axon extension, a process required for proper development of the lateral line circuit. In addition to elucidating some of the molecular cascades critical for cell shape changes, these results also raise additional questions and have important implications for global understanding of cell shape transitions.

Apical constriction is an evolutionarily conserved cell shape change, reiterated in multiple organ systems and species: it is required for formation of the vertebrate ear and neural tube and during drosophila eye formation, to name a few examples. While the cytoskeletal machinery that drives apical constriction is relatively well understood, the molecular cues that trigger cytoskeletal activation are not clear. Our work shows that the Fgf signaling pathway triggers intracellular cascades that activate the cytoskeleton. Because a similar understanding of the extracellular signals that coordinate apical constriction in other contexts are largely undiscovered, it will be important to determine whether activation of RTKs serves as a conserved mechanism of activating the

cytoskeleton or, more generally, apical constriction. In support of this idea, activation of the RTK EgfR is required for apical constriction during formation of the *Drosophila* morphogenetic furrow (Brown et al., 2006), suggesting that activation of RTKs may be a general mechanism of activating apical constriction.

Before cells constrict, their cytoskeletal machinery needs to be properly organized at the apical side. Our study begs the question: how are signals that drive polarized cytoskeletal assembly and activation of the cytoskeleton coordinated? Our and other studies show that just prior to apical constriction cells are synchronized such that their core cytoskeletal components are asymmetrically assembled in the apical domains of cells. In other words, a cell collective becomes poised just prior to apical constriction. Presumably, there is a mechanism for regulating timing and ensuring that the cytoskeleton is recruited prior to activation of constriction. Our study showed that FgfR-MAPK pathway, while required for the constriction, was not necessary for polarizing the cytoskeleton of the primordium cells. This observation implies that the signals that polarize the cytoskeleton and those that induce transcription must be distinct. Indeed, in the ventrolateral ectoderm and tracheal system of *Drosophila*, distinct molecular regulators of cytoskeletal recruitment have begun to be identified (Bertet et al., 2009; Letizia et al., 2011, respectively). The degree of conservation among these signals will also be interesting to understand in the future, as it may reveal an additional conserved process among species and organ systems that undergo apical constriction. Our study and future studies will contribute to an understanding of what goes wrong on the molecular level when

apical constriction fails, resulting in clinical presentations including neural tube defects.

In chapter 2, we propose a model in which a scaffold protein Jip3 is required for retrograde transport of the RTK Ret. While many RTKs are retrogradely transported, the physiological importance of retrograde transport in axon outgrowth is poorly understood. Current understanding of the physiological role of retrograde transport of RTKs is mainly based on studies of Trk-containing endosomes: Retrograde transport of these signaling endosomes is required for axon extension and neuronal survival (Heerssen et al., 2004; Wu et al., 2007). Though Ret is also retrogradely transported and Ret expression has been linked to neuronal survival and outgrowth, the specific relationship between retrograde transport and neuronal survival/outgrowth is not yet clear. Ret receptor activation may have a local role in growth cones, as well as actions in the cell body, following retrograde delivery to the soma.

Elucidation of the molecular signals downstream of Ret activation was beyond the scope of the study presented here. Additionally, whether these molecules are activated in the growth cone and/or cell body remains unclear. Nevertheless, our results strongly imply that Ret function is necessary for a complete axon extension. The similarity in axon outgrowth phenotypes between *ret* and *jip3* mutants suggest that Jip3-dependent retrograde transport of Ret is critical for the biological outcome of Ret signaling in the lateral line. Interestingly, loss of either Jip3 or Ret results in a relatively late impairment in axon outgrowth, potentially corresponding to the duration of time required to transport Ret from

the growth cone to cell body. If this late truncation indeed corresponds to the length of Ret's retrograde journey, it would suggest activation of a downstream pathway in the cell body, potentially transcriptional. Additionally, this role for Ret transport/signaling would also suggest that early axon outgrowth does not require Ret, possibly due to the existence of a second signaling pathway that facilitates early outgrowth. If true, this model would suggest that receptor-adaptor pairs are critical for discrete stages of axon outgrowth. Future experiments are necessary to distinguish these potential mechanisms of Ret signaling.

Together, these studies elucidate the upstream molecular control of cell shape changes. Both studies utilize the distinct advantages of the developing zebrafish lateral line system to understand different aspects of cell shape transitions, as well as raise additional questions about these processes. While some of these questions can be partially answered by further experimentation during zebrafish mechanosensory development, a more comprehensive understanding of cell shape will emerge as studies in other models are completed and compared to the data presented in this dissertation. When combined with previous literature, this dissertation contributes to a more comprehensive understanding of molecular steps required for development of the sensory systems in vertebrates.

REFERENCES

- Abramoff, M. D.** (2004). Image Processing with ImageJ. *Biophotonics international* **11**, 36–42.
- Aman, A. and Piotrowski, T.** (2008). Wnt/beta-catenin and Fgf signaling control collective cell migration by restricting chemokine receptor expression. *Dev. Cell* **15**, 749–761.
- Aman, A., Nguyen, M. and Piotrowski, T.** (2011). Wnt/ β -catenin dependent cell proliferation underlies segmented lateral line morphogenesis. *Dev. Biol.* **349**, 470–482.
- Amano, M., Nakayama, M. and Kaibuchi, K.** (2010). Rho-kinase/ROCK: A key regulator of the cytoskeleton and cell polarity. *Cytoskeleton (Hoboken)* **67**, 545–554.
- Andermann, P., Ungos, J. and Raible, D. W.** (2002). Neurogenin1 defines zebrafish cranial sensory ganglia precursors. *Dev. Biol.* **251**, 45–58.
- Bement, W. M., Forscher, P. and Mooseker, M. S.** (1993). A novel cytoskeletal structure involved in purse string wound closure and cell polarity maintenance. *J. Cell Biol.* **121**, 565–578.
- Beurg, M., Nam, J.-H., Crawford, A. and Fettiplace, R.** (2008). The actions of calcium on hair bundle mechanics in mammalian cochlear hair cells. *Biophys. J.* **94**, 2639–2653.

- Boldajipour, B., Mahabaleshwar, H., Kardash, E., Reichman-Fried, M., Blaser, H., Minina, S., Wilson, D., Xu, Q. and Raz, E.** (2008). Control of chemokine-guided cell migration by ligand sequestration. *Cell* **132**, 463–473.
- Breau, M. A., Wilson, D., Wilkinson, D. G. and Xu, Q.** (2012). Chemokine and Fgf signalling act as opposing guidance cues in formation of the lateral line primordium. *Development* **139**, 2246–2253.
- Brown, H. M., Van Epps, H. A., Goncharov, A., Grant, B. D. and Jin, Y.** (2009). The JIP3 scaffold protein UNC-16 regulates RAB-5 dependent membrane trafficking at *C. elegans* synapses. *Dev Neurobiol* **69**, 174–190.
- Cavalli, V., Kujala, P., Klumperman, J. and Goldstein, L. S. B.** (2005). Sunday Driver links axonal transport to damage signaling. *J. Cell Biol.* **168**, 775–787.
- Cernuda-Cernuda, R. and García-Fernández, J. M.** (1996). Structural diversity of the ordinary and specialized lateral line organs. *Microsc. Res. Tech.* **34**, 302–312.
- Chitnis, A. B., Nogare, D. D. and Matsuda, M.** (2012). Building the posterior lateral line system in zebrafish. *Developmental Neurobiology* **72**, 234–255.

- Drerup, C. M. and Nechiporuk, A. V.** (2013). JNK-interacting protein 3 mediates the retrograde transport of activated c-Jun N-terminal kinase and lysosomes. *PLoS Genet.* **9**, e1003303.
- Ernst, S., Liu, K., Agarwala, S., Moratscheck, N., Avci, M. E., Nogare, D. D., Chitnis, A. B., Ronneberger, O. and Lecaudey, V.** (2012). Shroom3 is required downstream of FGF signalling to mediate proneuromast assembly in zebrafish. *Development* **139**, 4571–4581.
- Faucherre, A., Pujol-Martí, J., Kawakami, K. and López-Schier, H.** (2009). Afferent Neurons of the Zebrafish Lateral Line Are Strict Selectors of Hair-Cell Orientation. *PLoS ONE* **4**, e4477.
- Ghysen, A. and Dambly-Chaudière, C.** (2007). The lateral line microcosmos. *Genes Dev.* **21**, 2118–2130.
- Gilmour, D., Knaut, H., Maischein, H.-M. and Nüsslein-Volhard, C.** (2004). Towing of sensory axons by their migrating target cells in vivo. *Nat. Neurosci.* **7**, 491–492.
- Gompel, N., Dambly-Chaudière, C. and Ghysen, A.** (2001). Neuronal differences prefigure somatotopy in the zebrafish lateral line. *Development* **128**, 387–393.
- Grandel, H., Draper, B. W. and Schulte-Merker, S.** (2000). dackel acts in the ectoderm of the zebrafish pectoral fin bud to maintain AER signaling. *Development* **127**, 4169–4178.

- Haas, P. and Gilmour, D.** (2006). Chemokine signaling mediates self-organizing tissue migration in the zebrafish lateral line. *Dev. Cell* **10**, 673–680.
- Haines, L., Neyt, C., Gautier, P., Keenan, D. G., Bryson-Richardson, R. J., Hollway, G. E., Cole, N. J. and Currie, P. D.** (2004). Met and Hgf signaling controls hypaxial muscle and lateral line development in the zebrafish. *Development* **131**, 4857–4869.
- Harding, M. J. and Nechiporuk, A. V.** (2012). Fgfr-Ras-MAPK signaling is required for apical constriction via apical positioning of Rho-associated kinase during mechanosensory organ formation. *Development* **139**, 3130–3135.
- Hava, D., Forster, U., Matsuda, M., Cui, S., Link, B. A., Eichhorst, J., Wiesner, B., Chitnis, A. and Abdelilah-Seyfried, S.** (2009). Apical membrane maturation and cellular rosette formation during morphogenesis of the zebrafish lateral line. *J. Cell. Sci.* **122**, 687–695.
- Huang, S.-H., Duan, S., Sun, T., Wang, J., Zhao, L., Geng, Z., Yan, J., Sun, H.-J. and Chen, Z.-Y.** (2011). JIP3 mediates TrkB axonal anterograde transport and enhances BDNF signaling by directly bridging TrkB with kinesin-1. *J. Neurosci.* **31**, 10602–10614.
- Ishiuchi, T. and Takeichi, M.** (2011). Willin and Par3 cooperatively regulate epithelial apical constriction through aPKC-mediated ROCK phosphorylation. *Nat. Cell Biol.* **13**, 860–866.

- Itoh, M. and Chitnis, A. B.** (2001). Expression of proneural and neurogenic genes in the zebrafish lateral line primordium correlates with selection of hair cell fate in neuromasts. *Mech. Dev.* **102**, 263–266.
- Jiao, L., Zhang, Y., Hu, C., Wang, Y.-G., Huang, A. and He, C.** (2011). Rap1GAP interacts with RET and suppresses GDNF-induced neurite outgrowth. *Cell Res.* **21**, 327–337.
- Kardon, J. R. and Vale, R. D.** (2009). Regulators of the cytoplasmic dynein motor. *Nat. Rev. Mol. Cell Biol.* **10**, 854–865.
- Kazmierczak, P., Sakaguchi, H., Tokita, J., Wilson-Kubalek, E. M., Milligan, R. A., Müller, U. and Kachar, B.** (2007). Cadherin 23 and protocadherin 15 interact to form tip-link filaments in sensory hair cells. *Nature* **449**, 87–91.
- Kelkar, N., Delmotte, M.-H., Weston, C. R., Barrett, T., Sheppard, B. J., Flavell, R. A. and Davis, R. J.** (2003). Morphogenesis of the telencephalic commissure requires scaffold protein JNK-interacting protein 3 (JIP3). *Proc. Natl. Acad. Sci. U.S.A.* **100**, 9843–9848.
- Knight, R. D., Mebus, K., D' Angelo, A., Yokoya, K., Heanue, T. and Roehl, H.** (2011). Ret signalling integrates a craniofacial muscle module during development. *Development* **138**, 2015–2024.
- Kwan, K. M., Fujimoto, E., Grabher, C., Mangum, B. D., Hardy, M. E., Campbell, D. S., Parant, J. M., Yost, H. J., Kanki, J. P. and Chien, C.-**

- B.** (2007). The Tol2kit: a multisite gateway-based construction kit for Tol2 transposon transgenesis constructs. *Dev. Dyn.* **236**, 3088–3099.
- Laguerre, L., Ghysen, A. and Dambly-Chaudière, C.** (2009). Mitotic patterns in the migrating lateral line cells of zebrafish embryos. *Developmental Dynamics* **238**, 1042–1051.
- Laranjeira, C. and Pachnis, V.** (2009). Enteric nervous system development: Recent progress and future challenges. *Auton Neurosci* **151**, 61–69.
- Lecaudey, V., Cakan-Akdogan, G., Norton, W. H. J. and Gilmour, D.** (2008). Dynamic Fgf signaling couples morphogenesis and migration in the zebrafish lateral line primordium. *Development* **135**, 2695–2705.
- Lee, Y., Hami, D., De Val, S., Kagermeier-Schenk, B., Wills, A. A., Black, B. L., Weidinger, G. and Poss, K. D.** (2009). Maintenance of blastemal proliferation by functionally diverse epidermis in regenerating zebrafish fins. *Dev. Biol.* **331**, 270–280.
- Lloyd, T. E., Machamer, J., O’Hara, K., Kim, J. H., Collins, S. E., Wong, M. Y., Sahin, B., Imlach, W., Yang, Y., Levitan, E. S., et al.** (2012). The p150(Glued) CAP-Gly domain regulates initiation of retrograde transport at synaptic termini. *Neuron* **74**, 344–360.
- López-Schier, H. and Hudspeth, A. J.** (2006). A two-step mechanism underlies the planar polarization of regenerating sensory hair cells. *Proc. Natl. Acad. Sci. U.S.A.* **103**, 18615–18620.

- Ma, E. Y., Rubel, E. W. and Raible, D. W.** (2008). Notch Signaling Regulates the Extent of Hair Cell Regeneration in the Zebrafish Lateral Line. *J. Neurosci.* **28**, 2261–2273.
- Matsuda, M., Dalle Nogare, D., Somers, K., Martin, K., Wang, C. and Chitnis, A. B.** (2013). Lef1 regulates Dusp6 to influence neuromast formation and spacing in the zebrafish posterior lateral line primordium. *Development.*
- McGraw, H. F., Drerup, C. M., Culbertson, M. D., Linbo, T., Raible, D. W. and Nechiporuk, A. V.** (2011). Lef1 is required for progenitor cell identity in the zebrafish lateral line primordium. *Development* **138**, 3921–3930.
- McKeown, S. J., Stamp, L., Hao, M. M. and Young, H. M.** (2013). Hirschsprung disease: a developmental disorder of the enteric nervous system. *Wiley Interdiscip Rev Dev Biol* **2**, 113–129.
- Metcalfe, W. K.** (1985). Sensory neuron growth cones comigrate with posterior lateral line primordial cells in zebrafish. *J. Comp. Neurol.* **238**, 218–224.
- Mohammadi, M., McMahon, G., Sun, L., Tang, C., Hirth, P., Yeh, B. K., Hubbard, S. R. and Schlessinger, J.** (1997). Structures of the tyrosine kinase domain of fibroblast growth factor receptor in complex with inhibitors. *Science* **276**, 955–960.
- Moughamian, A. J. and Holzbaur, E. L. F.** (2012). Dynactin is required for transport initiation from the distal axon. *Neuron* **74**, 331–343.

- Nechiporuk, A. and Raible, D. W.** (2008). FGF-dependent mechanosensory organ patterning in zebrafish. *Science* **320**, 1774–1777.
- Nicolson, T.** (2005). The Genetics of Hearing and Balance in Zebrafish. *Annual Review of Genetics* **39**, 9–22.
- Nishimura, T. and Takeichi, M.** (2008). Shroom3-mediated recruitment of Rho kinases to the apical cell junctions regulates epithelial and neuroepithelial planar remodeling. *Development* **135**, 1493–1502.
- Obholzer, N., Wolfson, S., Trapani, J. G., Mo, W., Nechiporuk, A., Busch-Nentwich, E., Seiler, C., Sidi, S., Söllner, C., Duncan, R. N., et al.** (2008). Vesicular glutamate transporter 3 is required for synaptic transmission in zebrafish hair cells. *J. Neurosci.* **28**, 2110–2118.
- Ortiz-Hidalgo, C.** (1992). Pol André Bouin, MD (1870-1962). Bouin's fixative and other contributions to medicine. *Arch. Pathol. Lab. Med.* **116**, 882–884.
- Plageman, T. F., Jr, Chauhan, B. K., Yang, C., Jaudon, F., Shang, X., Zheng, Y., Lou, M., Debant, A., Hildebrand, J. D. and Lang, R. A.** (2011). A Trio-RhoA-Shroom3 pathway is required for apical constriction and epithelial invagination. *Development* **138**, 5177–5188.
- Pujol-Martí, J., Zecca, A., Baudoin, J.-P., Faucherre, A., Asakawa, K., Kawakami, K. and López-Schier, H.** (2012). Neuronal birth order identifies a dimorphic sensorineural map. *J. Neurosci.* **32**, 2976–2987.

- Pullikuth, A. K. and Catling, A. D.** (2010). Extracellular signal-regulated kinase promotes Rho-dependent focal adhesion formation by suppressing p190A RhoGAP. *Mol. Cell. Biol.* **30**, 3233–3248.
- Raible, F. and Brand, M.** (2001). Tight transcriptional control of the ETS domain factors Erm and Pea3 by Fgf signaling during early zebrafish development. *Mech. Dev.* **107**, 105–117.
- Raible, D. W. and Kruse, G. J.** (2000). Organization of the lateral line system in embryonic zebrafish. *The Journal of Comparative Neurology* **421**, 189–198.
- Richardson, D. S., Lai, A. Z. and Mulligan, L. M.** (2006). RET ligand-induced internalization and its consequences for downstream signaling. *Oncogene* **25**, 3206–3211.
- Richardson, D. S., Rodrigues, D. M., Hyndman, B. D., Crupi, M. J. F., Nicolescu, A. C. and Mulligan, L. M.** (2012). Alternative splicing results in RET isoforms with distinct trafficking properties. *Mol. Biol. Cell* **23**, 3838–3850.
- Sai, X. and Ladher, R. K.** (2008). FGF signaling regulates cytoskeletal remodeling during epithelial morphogenesis. *Curr. Biol.* **18**, 976–981.
- Sapède, D., Rossel, M., Dambly-Chaudière, C. and Ghysen, A.** (2005). Role of SDF1 chemokine in the development of lateral line efferent and facial motor neurons. *Proc. Natl. Acad. Sci. U.S.A.* **102**, 1714–1718.

- Sawyer, J. M., Harrell, J. R., Shemer, G., Sullivan-Brown, J., Roh-Johnson, M. and Goldstein, B.** (2010). Apical constriction: a cell shape change that can drive morphogenesis. *Dev. Biol.* **341**, 5–19.
- Scholpp, S., Groth, C., Lohs, C., Lardelli, M. and Brand, M.** (2004). Zebrafish *fgfr1* is a member of the *fgf8* synexpression group and is required for *fgf8* signalling at the midbrain-hindbrain boundary. *Dev. Genes Evol.* **214**, 285–295.
- Schuster, K., Dambly-Chaudière, C. and Ghysen, A.** (2010). Glial cell line-derived neurotrophic factor defines the path of developing and regenerating axons in the lateral line system of zebrafish. *Proc. Natl. Acad. Sci. U.S.A.* **107**, 19531–19536.
- Shepherd, I. T., Pietsch, J., Elworthy, S., Kelsh, R. N. and Raible, D. W.** (2004). Roles for GFRalpha1 receptors in zebrafish enteric nervous system development. *Development* **131**, 241–249.
- Somlyo, A. P. and Somlyo, A. V.** (2003). Ca²⁺ sensitivity of smooth muscle and nonmuscle myosin II: modulated by G proteins, kinases, and myosin phosphatase. *Physiol. Rev.* **83**, 1325–1358.
- Sun, T., Yu, N., Zhai, L.-K., Li, N., Zhang, C., Zhou, L., Huang, Z., Jiang, X.-Y., Shen, Y. and Chen, Z.-Y.** (2013). c-Jun NH₂-terminal kinase (JNK)-interacting protein-3 (JIP3) regulates neuronal axon elongation in a kinesin- and JNK-dependent manner. *J. Biol. Chem.* **288**, 14531–14543.

Suzuki, A. and Ohno, S. (2006). The PAR-aPKC system: lessons in polarity. *J. Cell. Sci.* **119**, 979–987.

Suzuki, A., Arikawa, C., Kuwahara, Y., Itoh, K., Watanabe, M., Watanabe, H., Suzuki, T., Funakoshi, Y., Hasegawa, H. and Kanaho, Y. (2010). The scaffold protein JIP3 functions as a downstream effector of the small GTPase ARF6 to regulate neurite morphogenesis of cortical neurons. *FEBS Lett.* **584**, 2801–2806.

Suzuki, M., Morita, H. and Ueno, N. (2012). Molecular mechanisms of cell shape changes that contribute to vertebrate neural tube closure. *Dev. Growth Differ.* **54**, 266–276.

Tahira, T., Ishizaka, Y., Itoh, F., Sugimura, T. and Nagao, M. (1990). Characterization of ret proto-oncogene mRNAs encoding two isoforms of the protein product in a human neuroblastoma cell line. *Oncogene* **5**, 97–102.

Tsang, M. and Dawid, I. B. (2004). Promotion and attenuation of FGF signaling through the Ras-MAPK pathway. *Sci. STKE* **2004**, pe17.

Tsui, C. C. and Pierchala, B. A. (2010). The differential axonal degradation of Ret accounts for cell-type-specific function of glial cell line-derived neurotrophic factor as a retrograde survival factor. *J. Neurosci.* **30**, 5149–5158.

- Ungos, J. M., Karlstrom, R. O. and Raible, D. W.** (2003). Hedgehog signaling is directly required for the development of zebrafish dorsal root ganglia neurons. *Development* **130**, 5351–5362.
- Valdivia, L. E., Young, R. M., Hawkins, T. A., Stickney, H. L., Cavodeassi, F., Schwarz, Q., Pullin, L. M., Villegas, R., Moro, E., Argenton, F., et al.** (2011). Lef1-dependent Wnt/ β -catenin signalling drives the proliferative engine that maintains tissue homeostasis during lateral line development. *Development* **138**, 3931–3941.
- Vicente-Manzanares, M., Ma, X., Adelstein, R. S. and Horwitz, A. R.** (2009). Non-muscle myosin II takes centre stage in cell adhesion and migration. *Nat. Rev. Mol. Cell Biol.* **10**, 778–790.
- Villablanca, E. J., Renucci, A., Sapède, D., Lec, V., Soubiran, F., Sandoval, P. C., Dambly-Chaudière, C., Ghysen, A. and Allende, M. L.** (2006). Control of cell migration in the zebrafish lateral line: implication of the gene “tumour-associated calcium signal transducer,” *tacstd*. *Dev. Dyn.* **235**, 1578–1588.
- Von Trotha, J. W., Campos-Ortega, J. A. and Reugels, A. M.** (2006). Apical localization of ASIP/PAR-3:EGFP in zebrafish neuroepithelial cells involves the oligomerization domain CR1, the PDZ domains, and the C-terminal portion of the protein. *Dev. Dyn.* **235**, 967–977.

- Wang, G., Cadwallader, A. B., Jang, D. S., Tsang, M., Yost, H. J. and Amack, J. D.** (2011). The Rho kinase Rock2b establishes anteroposterior asymmetry of the ciliated Kupffer's vesicle in zebrafish. *Development* **138**, 45–54.
- Weiser, D. C., Pyati, U. J. and Kimelman, D.** (2007). Gravin regulates mesodermal cell behavior changes required for axis elongation during zebrafish gastrulation. *Genes Dev.* **21**, 1559–1571.
- Westerfield, M.** (1995). *The Zebrafish Book. A Guide for the Laboratory Use of Zebrafish (Danio Rerio)*. 3rd ed. Eugene, OR: University of Oregon Press.
- Whitfield, T. T.** (2002). Zebrafish as a model for hearing and deafness. *Journal of Neurobiology* **53**, 157–171.
- Young, H. M., Anderson, R. B. and Anderson, C. R.** (2004). Guidance cues involved in the development of the peripheral autonomic nervous system. *Auton Neurosci* **112**, 1–14.